Dynamical mean-field theory of the small polaron

S. Ciuchi
Dipartimento di Fisica, Università de L'Aquila, via Vetoio, I-67100 Coppito-L'Aquila, Italy

F. de Pasquale and S. Fratini*
Dipartimento di Fisica, Università di Roma ''La Sapienza,'' piazzale Aldo Moro 5, I-00185 Roma, Italy

D. Feinberg
Laboratoire d'Etudes des Propriétés Electroniques des Solides, Centre National de la Recherche Scientifique, Boîte Postale 166, 38042 Grenoble Cedex 9, Grenoble, France

(Received 7 November 1996; revised manuscript received 25 March 1997)

A dynamical mean-field theory of the small polaron problem is presented, which becomes exact in the limit of infinite dimensions. The ground-state properties and the one-electron spectral function are obtained for a single electron interacting with Einstein phonons by a mapping of the lattice problem onto a polaronic impurity model. The one-electron propagator of the impurity model is calculated through a continued fraction expansion, at both zero and finite temperature, for any electron-phonon coupling and phonon energy. In contrast to the ground-state properties, such as the effective polaron mass, which show a continuous behavior as the coupling is increased, spectral properties exhibit a sharp qualitative change at low enough phonon frequency: beyond a critical coupling, one energy gap and then more open in the density of states at low energy, while the high-energy part of the spectrum is broad and can be qualitatively explained by a strong coupling adiabatic approximation. As a consequence, narrow and coherent low-energy subbands coexist with an incoherent featureless structure at high energy. The subbands denote the formation of quasiparticle polaron states. Also, divergencies of the self-energy may occur in the gaps. At finite temperature such an effect triggers an important damping and broadening of the polaron subbands. On the other hand, in the large phonon frequency regime such a separation of energy scales does not exist and the spectrum always has a multipeaked structure. [S0163-1829(97)06931-2]

I. INTRODUCTION: THE SINGLE POLARON PROBLEM

The polaron problem is an old but not fully solved problem of solid state physics. The *small polaron* theory, which will be considered here, assumes a short-range electron-phonon interaction and explicitly includes the lattice periodicity.[1,2] We therefore aim to study systems where screening is effective. This addresses, for instance, the situation of a metal consisting of different bands, one of them being narrow enough to allow for a strong coupling to phonons. In fact, if the crystal can be considered as being made of strongly deformable molecularlike units with narrow-band electrons hopping from one to another, then the conditions for a strong polaron effect can be realized.[2] In realistic structures, for example, transition-metal oxides or organic metals, such units exist that provide local (oscillation) phonon modes and are indeed strongly coupled to well-defined electronic orbitals. Recently, interest in polaron theory has been revived, due to important classes of materials, including the high-temperature superconductors[3] and the ''colossal'' magnetoresistance manganites.[4–6] In fact, in the insulating parent phase of superconducting cuprates, polarons have been unambiguously detected by optical measurements,[7–9] and some evidence of strong electron-phonon coupling effects has been given recently in the metallic phase.[9,10] In the manganites, on the other hand, strong static or dynamic Jahn-Teller distortions appear at the metal-insulator transitions.[4–6]

The problem of a single polaron becomes relevant for low carrier density, but also by itself, as a paradigm to study the effect of strong coupling electron-phonon interactions. In the intermediate and strong coupling regimes, the small polaron problem is already a nontrivial many-body problem:[11] the difficulty consists in describing the dressing of the electron by a coherent multiphonon cloud, moving coherently with it so as to form a quasiparticle. Perturbative techniques, starting either from the free-electron limit or from the atomic limit (strong coupling expansions)[2,12–15] fail to describe the dressing effect in the intermediate regimes. On the other hand, nonperturbative solutions based, for instance, on a variational ansatz[16–18] are expected to give reliable results only for ground-state properties, such as the effective polaron mass. But, to our knowledge, no satisfactory description of the full spectral properties has been obtained so far.

Holstein's molecular crystal model[2] involves tight-binding electrons coupled to dispersionless optical phonons. As a function of phonon frequency and electron-phonon coupling, it displays a variety of interesting regimes. The strong coupling regime leads to the formation of small polarons, with a dramatic increase of the effective mass for low phonon frequencies.[2,12] On the other hand, for exactly zero phonon frequency, an adiabatic solution can be obtained with self-trapping of the polarons appearing only above some critical coupling value, in dimensions greater than one.[17,19,20]

In this context, the recent discovery of a nonperturbative theory for interacting quantum problems, based on the limit

of infinite lattice coordination (or dimensionality),[38,46,21–24] opened a new way of attacking strong electron-phonon problems. A few recent papers have addressed the problem of superconductive and charge-density-wave instabilities of the metallic state, close to half filling, either in weak coupling,[25] using self-consistent techniques,[26,27] or from the local impurity method,[28] also including a local electron repulsion (the Holstein-Hubbard problem).[29] Also, a solution at finite density in the adiabatic limit (zero phonon frequency) was obtained.[30] On the other hand, exact results for the spectral function of a single polaron at zero temperature were recently reported by the authors.[31] The aim of the present work is to provide a complete description of the small polaron crossover based upon the knowledge of spectral quantities in the whole range of parameters and also at nonzero temperature. The most striking features are found in an intermediate coupling regime where no known approximation scheme works.

Similarly to the Hubbard model, the infinite-dimensional limit allows one to map the lattice problem onto a self-consistent local impurity model, here called ''polaron impurity.''[31,28] It consists of a single-site electron-phonon problem, embedded into a quantum effective medium characterized by an effective ''free'' propagator, which has to be self-consistently determined. This mapping preserves all the complexities of the quantum dynamics of the problem, namely, the interplay between electron and lattice fluctuations *at the local level*. The crucial point here is that for a single electron the impurity model can be *analytically* solved by a recursion formula for any noninteracting impurity propagator, leading to a *continued-fraction expansion* (CFE) solution for the fully dressed propagator. This unique feature allows one to obtain at the end an exact solution for the lattice problem in the limit of infinite dimensions. This solution provides directly, with modest computational efforts, the ground state as well as the spectral properties in the thermodynamic limit and at any temperature. Therefore it is somehow complementary to numerical works performed in finite dimensions, such as Monte Carlo simulations[20,32] or exact diagonalization of finite clusters.[33,34] Indeed, the former are limited to finite temperatures, and the latter have to deal with finite-size effects.

The main result of the present self-consistent impurity approach is that, in the crossover regime, low- and high-energy scales can be accurately described, as in the Mott-Hubbard transition problem.[24] Polaron states in the low-energy range appear as coherent strongly renormalized quasiparticle states, while at higher energies the electron is incoherently scattered by a quasiclassical random distortion. These features are clearly displayed in the low phonon frequency regime, where the spectral density displays low-energy peaks coexisting with a broad and incoherent high-energy continuum. This provides a physically transparent representation of the polaron crossover. As the coupling strength is increased, it proceeds through successive openings of gaps in the spectral density, separating polaron subbands. At intermediate couplings, and decreasing the phonon frequency, one finds that the dressing of electron states by a multiphonon coherent cloud drastically reduces the effective electronic energy scales and leads to an adiabaticity ''catastrophe'' in the low-energy spectrum. In terms of a perturbative expansion, this can be clearly ascribed to high-order vertex dressing. It is important to emphasize that even in an intermediate regime of couplings a well-defined polaron quasiparticle excitation is present at low energy. Also, an important feature is the appearance of a discrete set of frequencies where the self-energy diverges within the low-energy gaps of the spectrum. Those points are sensitive to disorder.[35] In particular, at finite temperatures, they enhance the damping and thermal broadening of polaron states in their vicinity, leading to a loss of coherence of the main polaron subband.

This paper is organized as follows. In Sec. II, we introduce the Holstein molecular crystal model and we discuss the main limiting cases in a finite-dimensional lattice. In Sec. III, we introduce the impurity analogy and the exact CFE solution of the impurity model, at zero and at finite temperature. In the same section the limiting results of the CFE are presented and compared to the finite-dimensional case. Section IV presents the general results of the CFE solution of the impurity problem. Section V is devoted to conclusions and to a discussion of possible extensions of this method to finite density, in relation with a coherent potential approximation (CPA) formulation of the CFE.

II. THE HOLSTEIN MODEL

In this section we shall summarize the main results concerning the Holstein model in finite dimensions, in the limit in which analytical calculations can be performed. We especially focus on the role of dimensionality, which will allow one to discuss later how our theory (exact in infinite dimensions) can be compared with results in finite-dimensional lattices.

The Holstein model consists of tight-binding conduction electrons interacting with local dispersionless phonon modes. The Hamiltonian is

$$H=-\sum_{\langle ij\rangle,\sigma} t_{i,j}(c^{\dagger}_{i,\sigma}c_{j,\sigma}+\text{H.c.})-g\sum_{i,\sigma} c^{\dagger}_{i,\sigma}c_{i,\sigma}(a_i+a_i^{\dagger}) + \omega_0\sum_i a_i^{\dagger}a_i, \tag{1}$$

where $c^{\dagger}_{i,\sigma}$ ($c_{i,\sigma}$) creates (destroys) an electron with spin σ at site i, and $a_i^{\dagger}$ (a_i) creates (destroys) a phonon at site i. The hopping matrix elements $t_{i,j}$ connect nearest-neighboring sites of a lattice in d dimensions and we assume they give rise to a band of half bandwidth t. This model possesses two independent control parameters.[18] The first one is the bare coupling constant $\lambda=g^2/\omega_0 t=|\epsilon_p|/t$, where $\epsilon_p=-g^2/\omega_0$ is the polaron energy obtained in the atomic limit ($t=0$). The second one is the adiabatic parameter $\gamma=\omega_0/t$. A third parameter can be conveniently introduced as a combination of the above ones, as $\alpha=g/\omega_0$, with $\alpha^2=\lambda/\gamma$. While λ and γ are commonly used as parameters in the perturbative analysis, the parameter α, which measures the strength of the lattice deformation involved in the polaron effect, will show to be crucial in the strong coupling regime. Let us stress that these parameters are defined from the bare energy scales ω_0, g, t in the Hamiltonian, contrarily to usual definitions in the theory of electron-phonon interaction in metals where in particular the dressed phonon frequency is used. It is worth

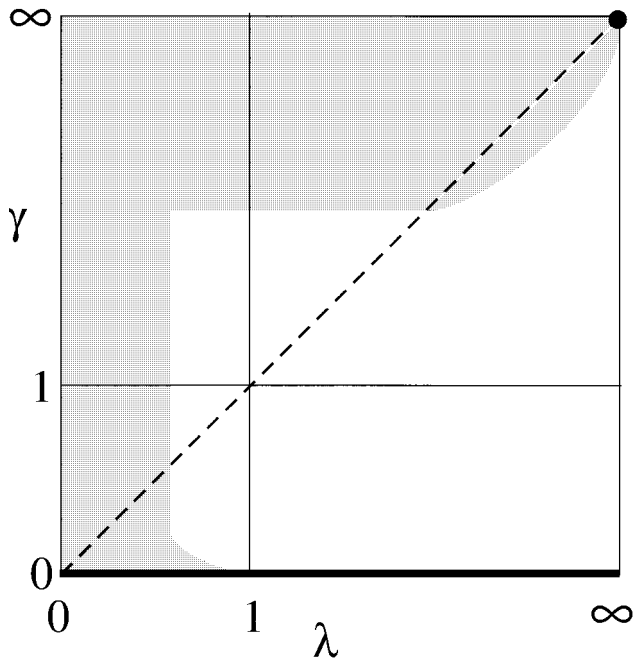

FIG. 1. A schematic plot of the regions of parameter space (λ,γ) for the Holstein model in an infinite-dimensional Bethe lattice. Below the dashed line ($\alpha^2=1$) multiphonon processes are important. On the bold horizontal axis the adiabatic limit holds. The point in the upper right corner is reached at the atomic $t=0$ limit. In the shaded area perturbation theory (small λ) or Holstein's approximation (large γ) are valid. Notice that perturbation theory extends its validity up to the adiabatic critical value for localization λ_c (see text).

defining the following regimes and limits, which are relevant to the Holstein model: (i) weak (strong) coupling $\lambda<1$ (>1); (ii) small (large) phonon frequency $\gamma<1$ (>1); (iii) multiphonon regime $\alpha^2>1$; (iv) adiabatic limit $\omega_0=0$, finite λ. Figure 1 shows the corresponding regions in the (λ,γ) plane.

Throughout this paper we shall concentrate on the problem of one electron in interaction with phonons, i.e., a system in which density is zero in the thermodynamic limit. To analyze the perturbative behavior of the model we shall first discuss the simplifications due to this limit. The discussion is restricted to the zero-temperature limit but can be easily generalized to finite temperatures (see Sec. II B). For a single electron the Green's function in the site representation can be defined as

$$G_{i,j}(t)=-i\langle 0|Tc_j(t)c_i^{\dagger}(0)|0\rangle, \tag{2}$$

where $|0\rangle$ is the vacuum for phonons and electrons and the unessential spin indices are omitted. One observes that there is only one possible ordering ($t>0$) of the T product, so that the function is purely retarded.[37] Then the standard perturbation theory is introduced in the site representation by defining the electron self-energy[38] $\Sigma_{i,j}(\omega)$ through the Dyson equation

$$G_{i,j}=[\mathcal{G}_0]_{i,j}+\sum_{k,l}[\mathcal{G}_0]_{i,k}\Sigma_{k,l}G_{l,j}, \tag{3}$$

where $\mathcal{G}_0$ is the free-electron propagator.

At zero density, the following simplifications hold: (i) A general self-energy diagram consists of a single electron line first emitting and then absorbing phonons. (ii) The emission (absorption) of a phonon consists in subtracting (adding) a quantum of phonon frequency ω_0 to the energy of the propagating electron line.

The first statement comes from the absence of density fluctuations in the zero density limit (no bubble diagrams, no phonon renormalization). Moreover, in the zero-temperature limit all the phonons must be created from vacuum before being absorbed. To illustrate the second statement, we first notice that in a generic self-energy diagram involving N phonon lines, it is always possible to choose an integration contour that avoids all the poles and cuts of the electron Green's function, since the retarded electron propagator is analytic in the upper half plane. Then the only contribution comes from the poles associated to the phonon lines.

A. Weak coupling and adiabatic limit

The perturbation expansion of the self-energy to second order in g gives a local (**k**-independent) self-energy:

$$\Sigma_2(\omega)=g^2\mathcal{G}_0(\omega-\omega_0), \tag{4}$$

where $\mathcal{G}_0$ is the local free propagator obtained by the knowledge of the free particle density of states (DOS) $N(\epsilon)$ as $\mathcal{G}_0=\int d\epsilon N(\epsilon)(\omega-\epsilon)^{-1}$. Notice that dimensionality enters only through the free DOS.[39] The electron effective mass, in the case of a local self-energy, is easily calculated via

$$\frac{m^*}{m}=1-\left.\frac{d\mathrm{Re}\Sigma(\omega)}{d\omega}\right|_{E_0}, \tag{5}$$

where E_0 is the ground-state energy.

Let us first consider the low phonon frequency regime. In this case for electron states lying at the bottom of a band, dimensionality effects enter through the band shape near the band bottom and control both the behavior of the effective mass and the spectral properties. We assume that near the band bottom ($\epsilon=-t$) $N(\epsilon)\sim(1+\epsilon/t)^{d/2-1}/t$, then one has from Eqs. (4) and (5) for $0<d<4$ (Ref. 40)

$$\frac{m^*}{m}=1+\lambda k_d\gamma^{d/2-1}, \tag{6}$$

where k_d is a numerical constant.[41] It is not surprising that we do not recover the expected ''Migdal'' result $1+\lambda$. In fact this last result is obtained by assuming an infinite flat band, which could be the case of a metal whose Fermi energy lies far from singularities (like Van Hove ones) in the DOS. From Eq. (6) we can define an effective coupling $\tilde{\lambda}=\lambda N(E_0+\omega_0)t$ as in the case of Van Hove singularities[42] in order to write $m^*/m=1+\tilde{\lambda}$. The effective coupling strength $\tilde{\lambda}$ tends to zero for vanishing phonon frequency in dimensions $d>2$ (keeping λ constant), while it goes to infinity for $d<2$. Surprisingly, a *perturbative* analysis provides nontrivial information about the adiabatic limit: for $d>2$ we expect free-electron behavior while for $d<2$ the perturbation expansion *around a delocalized solution* fails in the adiabatic limit for any finite λ. This is consistent with the nonperturbative findings of Ref. 19, where it is shown that renormal-

ization effects are absent up to a *finite* value of $\lambda=\lambda_c$ for $d\geqslant 2$, while in $d=1$ the behavior is polaronic for any finite value of λ.[43]

In the opposite case of large phonon frequency, calculating the self-energy in Eq. (4) for large ω_0 and taking advantage of the asymptotical behavior of the free propagator at high energy, it is easy to get

$$\frac{m^*}{m}=1+\alpha^2. \tag{7}$$

It appears as a first-order expansion in power of α^2. As we shall see this expansion is actually resummed, in the large-phonon-frequency limit, by the use of the Lang-Firsov[12] transformation.

It is worth comparing the spectral properties obtained at finite bandwidth and zero density with those derived up to second order in g in the classical work of Engelsberg and Schrieffer[39] in the case of an infinite bandwidth. Since the self-energy is local one can define the spectral function as a function of energy ϵ and frequency ω (Ref. 39)

$$A(\epsilon,\omega)=-\frac{1}{\pi}\mathrm{Im}\,\frac{1}{\omega-\epsilon-\Sigma(\omega)}, \tag{8}$$

where ϵ runs over the noninteracting band energies $\epsilon_{\mathbf{k}}$ of a translationally invariant lattice. The electron spectral density $\mathcal{N}(\omega)=-(1/\pi)\mathrm{Im}G(\omega)$ is derived from Eq. (8) by integrating over the energy distribution.

In agreement with Ref. 39, one easily obtains a quasiparticle excitation spectrum (with $\mathrm{Im}\Sigma=0$) at energies $E_0\leqslant\omega\leqslant E_0+\omega_0$ and an incoherent broad spectrum at larger energies.

In the low phonon frequency case the spectral density of the low-energy quasiparticle states can be determined by the low-energy properties of the free DOS. A band of coherent excitations could separate from incoherent states, depending on the dimensionality. The equation that determines the band edges is

$$\omega-\mathrm{Re}\Sigma(\omega)=\pm t. \tag{9}$$

The minus sign determines the band bottom *including the ground-state energy* while the plus sign determines the band top. Using the self-energy of Eq. (4) it is easy to see that near $E_0+\omega_0$, $\mathrm{Re}\Sigma$ diverges in $d=1$ and $d=2$ as $\omega^{-1/2}$ and $\ln(\omega)$, respectively, while it is well behaved for $d>2$. In contrast with Ref. 39 the finite-bandwidth effects taken into account by Eq. (9) generate a gap in $d=1,2$. More precisely the amplitude of the gap (in units of the bandwidth) between coherent and incoherent states scales with $(\lambda\gamma)^4$ in $d=1$ and with $\exp(-1/\lambda\gamma)$ in $d=2$. In $d=3$ the real part of the self-energy does not diverge at $E_0+\omega_0$ so that a sufficiently large coupling is necessary to fulfill Eq. (9). In this case we expect the appearance of a gap only for λ greater than a certain value, which depends on the phonon frequency and explicitly on the whole band shape.

The discussion of this subsection suggests that, in dimensions larger than 2, perturbative expansions fail beyond some critical coupling above which gaps open up in the one-electron density of states. This property will be revealed in detail by the self-consistent local impurity theory analyzed in Secs. III and IV.

B. Atomic and large-phonon-frequency limits

The *atomic* limit is defined as the zero hopping case ($t=0$). It can be understood also as an infinite coupling limit $\lambda\to\infty$. One considers a single electron on a single site lattice (atom) whose Hamiltonian is given by Eq. (1) with $t=0$. In the case of zero bandwidth the Hamiltonian of Eq. (1) can be diagonalized by the unitary Lang-Firsov (LF) transformation[12]

$$U=\exp[\alpha c^\dagger c(a-a^\dagger)]. \tag{10}$$

The effect of this transformation is to shift the phonon operators by a quantity α so that the electron-phonon interaction is eliminated. It introduces a new fermion, the polaron, which carries this phonon field shift

$$c\to Xc, \tag{11}$$

where $X=\exp\alpha(a-a^\dagger)$. Once the transformation is performed, the Hamiltonian becomes diagonal and the ground-state energy is the polaronic energy $\epsilon_p=-g^2/\omega_0$, the excited polaron states having an energy $\epsilon_p+n\omega_0$.

Due to the presence of an electron at a given site, the lattice is deformed. The magnitude of this effect is measured by the local part of the static electron-displacement correlation function defined as

$$C_0=\langle n_i(a_i+a_i^\dagger)\rangle. \tag{12}$$

In the atomic limit one gets $C_0=2\alpha$, which means that the atomic ground state is that of a localized polaron, i.e., an electron surrounded by a ''cloud'' represented by a coherent (Glauber) phonon state, with an average number $\langle a^\dagger a\rangle=\alpha^2$ of phonons. The electron propagator can also be calculated after the LF transformation[37]

$$G(\omega)=\sum_{n=0}^{\infty}\frac{\alpha^{2n}e^{-\alpha^2}}{n!}\,\frac{1}{\omega-n\omega_0-\epsilon_p}. \tag{13}$$

The resulting spectral density appears as a Poissonian distribution of δ peaks separated by the phonon frequency ω_0. By exploiting the Lehmann representation of the Green's function one can see that such a distribution is due to the projection of a localized zero-phonon state onto the (n-phonon) polaron eigenstates of the Hamiltonian. This can be usefully understood from a gedanken x-ray or optical absorption experiment, where the wave function of the localized electronic final state (with undistorted lattice) is expanded onto the (lattice relaxed) polaron eigenstates, which builds the electron spectral function. From Eq. (13) we see that the Green's function has a spectral weight close to the ground-state energy that is exponentially small in the interaction strength, while the spectral weight is maximum for excitations involving approximately $n\sim\alpha^2$ phonons.

Let us now consider the action of the hopping. An approximation valid for large phonon frequencies is derived from the LF transformation, applied to the Hamiltonian with

a nonzero hopping term. The hopping term, modified by the transformation, represents the hopping of the *polaron*:

$$t_{i,j}c^{\dagger}_{i,\sigma}c_{j,\sigma}\rightarrow t_{i,j}X^{\dagger}_{i}X_{j}c^{\dagger}_{i,\sigma}c_{j,\sigma}. \tag{14}$$

The Holstein approximation[2] consists in averaging the polaron kinetic energy on the free phonon variables, thus obtaining at zero temperature an effective hopping amplitude

$$t_{i,j}\langle 0|X^{\dagger}_{i}X_{j}|0\rangle = t_{i,j}e^{-\alpha^2} \tag{15}$$

for i,j nearest neighbors. This approximation amounts to neglecting phonon emission and absorption during the hopping process. It is believed to give correct results when ω_0 is the largest energy scale.[44]

In the same spirit, following Alexandrov and Ranninger, one can go further and use the same approximation to calculate the *electron* propagator, also for finite electron density,[13] which gives

$$A(\epsilon_k,\omega) = -\frac{1}{\pi}\mathrm{Im}\left[\frac{e^{-\alpha^2}}{\omega-\epsilon^{*}_{k}-\epsilon_p}+\sum_{n=1}^{\infty}\frac{1}{N}\sum_{q}\frac{\alpha^{2n}e^{-\alpha^2}}{n!}\times\frac{1}{\omega-\epsilon^{*}_{q}-n\omega_0-\epsilon_p}\right], \tag{16}$$

where $\epsilon^{*}_{k}=\epsilon_k\exp(-\alpha^2)$ runs over the renormalized bandwidth obtained by replacing the free hopping parameter t by $t^{*}=t\exp(-\alpha^2)$. This solution shows a coherent low-energy quasiparticle band describing a polaron of effective mass

$$\frac{m^{*}}{m}=e^{\alpha^2} \tag{17}$$

located around ϵ_p, together with an incoherent structure at higher energies.

Let us give a physical interpretation of this result by showing that at least for the low-energy states it corresponds to substituting the exact self-energy with the atomic one. This is valid in the case $\omega_0 \gg t$ where a generic scattering process will lead electrons through intermediate states out of the band. In this scattering process the system can be thought of as a flat band ''atomic'' system in interaction with high-energy phonons. For frequencies near the polaron ground-state energy ϵ_p, the atomic self-energy reads

$$\Sigma(\omega)=\omega(1-e^{\alpha^2})+e^{\alpha^2}\epsilon_p. \tag{18}$$

Using the definition Eq. (8) we get the spectral function

$$A(\epsilon,\omega)=-\frac{1}{\pi}\mathrm{Im}\frac{e^{-\alpha^2}}{\omega-\epsilon^{*}-\epsilon_p}, \tag{19}$$

where $\epsilon^{*}=\epsilon\exp(-\alpha^2)$ describes the renormalized band. Thus one recovers the low energy part of Eq. (16) from an approximation to the self-energy that is justified in the large phonon frequency regime and *near the quasiparticle polaronic peak*. However, for $\alpha^2 \gg 1$, i.e., when multiphonon effects are important, the validity of the Holstein approximation is questionable even in the case of large *but finite* phonon frequency. Results from small cluster exact diagonalization[45] show that the adiabatic ratio ω_0/t must increase as α^2 to ensure the validity of the Holstein approximations (see Fig. 1).

Finally, let us give the result for the electron propagator in the atomic limit, at finite temperature. The Green's function is then defined generally by averaging on phonons only (the problem is that of a ''cold'' electron in a thermalized phonon bath). In the atomic limit, it is obtained in the same way as at $T=0$, yielding the pole representation[37]

$$G(\omega)=\sum_{n=-\infty}^{+\infty}e^{-(2N+1)\alpha^2}I_n\{2\alpha^2[N(N+1)]^{1/2}\}\times e^{n\omega_0/2T}\frac{1}{\omega-n\omega_0-\epsilon_p}, \tag{20}$$

where $N=\exp(-\omega_0/T)$ is the phonon thermal weight and $I_n\{z\}$ are the Bessel functions of complex argument.

Comparing this expression with Eq. (13), we remark that at $T\neq 0$ the corresponding spectral function displays peaks at frequencies below the polaron ground-state energy, with a spectral weight that is exponentially small at low temperatures. This apparent paradox of having electron states at *lower* energy than the ground state can be explained if one interprets these states as polaron states formed after absorbing n thermal phonons from the thermal bath, with a probability $\exp(-\beta n\omega_0/2)$. This reduces the cost in lattice energy required to form the polaron. Since the polaron energy results from a balance between this (positive) cost and the (negative) electron-lattice coupling energy, it is possible to create states lying below the zero-temperature ground-state level. The price to be paid is that these states are incoherent, due to the incoherent (thermal) phonon distribution. Also, the chemical potential goes to minus infinity, allowing the fermion occupation number to be zero at any energy for one particle at finite T.

III. THE IMPURITY ANALOGY AND THE EXACT SOLUTION FOR A SINGLE ELECTRON

The dynamical mean-field theory is developed as the exact solution of an infinite-dimensional[46] or infinite connectivity lattice. It has been shown[38,46] that to have a finite free-electron kinetic energy the hopping matrix elements must be scaled with the square root of the lattice dimensionality or lattice coordination.[36] A second point to deal with is the proper choice of the infinite coordination lattice in order to get a finite value of the ground-state energy. In fact, a problem arises, for example, in the case of a hypercubic lattice, which has a Gaussian DOS with an infinite tail towards low energy.[46] For large but finite dimensions the scaling of the hopping matrix elements implies that the ground-state energy of one electron is proportional to $\sqrt{d}$. Therefore, the formation of a small polaron requires an electron-phonon coupling energy of the same order of magnitude and a coupling constant λ, which diverges with $\sqrt{d}$. Indeed, just like the formation of a bound state from an external potential, polaron formation by self-trapping requires an infinite coupling strength in an ordinarily connected lattice in infinite dimensions (see Ref. 31). To overcome this difficulty we consider a Bethe lattice of infinite coordination d. The hopping matrix ele-

ments in Eq. (1) have been scaled as $t_{i,j}=t/2\sqrt{d}$ with t being the half bandwidth of the lattice. In the Bethe lattice (see Ref. 47, Sec. 5.3.4) only self-retracing paths are allowed. A restriction of the possible paths to go from one site to another allows this lattice to mimic a finite-dimensional one also in the limit of infinite coordination, giving rise to a finite bandwidth semielliptical free DOS,

$$N(\epsilon)=\frac{2}{\pi t^2}\sqrt{t^2-\epsilon^2}, \tag{21}$$

which correctly simulates the low-energy features of a three-dimensional lattice. More generally, in interacting fermion problems, with this particular choice, localization phenomena can be found even in the infinite-dimension limit; for instance, the Mott-Hubbard transition is correctly obtained at a finite coupling for the half-filled Hubbard model.[24]

Let us now come to the essential simplification occurring in the limit of infinite dimensions, namely, the fact that the electron self-energy is *local* in space. The usual argument that holds for local electron interactions[46,22,51] can be worked out also in the context of the Holstein model. One can carry on the standard argument but taking into account also the phonon self-energies and electron-phonon vertices instead of the electron-electron four leg vertices.[46] This gives the scaling of the real-space propagator with the intersite ''Manhattan'' distance $R=|i-j|$ as $G(R)\propto 1/\sqrt{d}^R$. Using this scaling and the skeleton expansion of the vertex function one can prove that the self-energy is not only local but that it *depends only on local phonon and electron propagators*.[46,24] In practice in a generic self-energy diagram all the internal lines are local propagators.

Using the locality of the self-energy, the lattice propagator in the k space is then given by $G_{\mathbf{k}}(\omega)=[\omega-\epsilon_{\mathbf{k}}-\Sigma(\omega)]^{-1}$, where $\epsilon_{\mathbf{k}}$ is the tight-binding electronic dispersion. Writing $G_{ii}=1/N\Sigma_{\mathbf{k}}G_{\mathbf{k}}$ and introducing the free DOS as $N(\epsilon)=1/N\Sigma_{\mathbf{k}}\delta(\epsilon-\epsilon_{\mathbf{k}})$ one has (dropping the site index for $i=j$)

$$G(\omega)=\int d\epsilon\frac{N(\epsilon)}{\omega-\Sigma(\omega)-\epsilon}. \tag{22}$$

Notice that in infinite dimensions the properties of the lattice enter only through the free-electron DOS.

Having a local self-energy, one can demonstrate following Ref. 22 the existence of an impurity model equivalent to the lattice problem. This can be readily seen by writing the real-space Dyson equation for the *local* propagator G_{ii} [Eq. (3)] in two steps. The first one involves self-energy contributions on sites j, with $j\neq i$. Once these contributions are resummed, one is led with a modified local propagator, denoted by G_0. The latter can be used in the full Dyson equation for G_{ii}, reintroducing the missing self-energy contributions that involve *the same site i*. It leads to the *local* Dyson equation for $G_{ii}=G$ (assuming translational symmetry)

$$G(\omega)=[G_0^{-1}(\omega)-\Sigma(\omega)]^{-1}. \tag{23}$$

The problem is therefore that of an impurity embedded into a medium. All the electron-phonon scattering processes occurring on sites other than the impurity site are contained in the effective ''free'' impurity propagator G_0, while local processes at the impurity site are taken into account by the self-energy Σ in Eq. (23).

This impurity problem can be made more physical by parametrizing it as a ''polaron'' Anderson impurity model involving a localized ''d'' level coupled to a local phonon, and hybridized with a fictitious conduction electron band ''c'' of dispersion $E_{\mathbf{k}}$:

$$H_{\mathrm{imp}}=\sum_k E_{\mathbf{k}}c_{\mathbf{k}}^{\dagger}c_k-\sum_k V_{\mathbf{k}}(c_{\mathbf{k}}^{\dagger}d+d^{\dagger}c_k)+\omega_0 a^{\dagger}a - g d^{\dagger}d(a+a^{\dagger}), \tag{24}$$

with new impurity parameters $V_{\mathbf{k}}$ and $E_{\mathbf{k}}$ being related to the propagator G_0 by

$$G_0^{-1}(\omega)=\omega-\int_{-\infty}^{+\infty}dE\frac{\Delta(E)}{\omega-E} \tag{25}$$

and

$$\Delta(E)=\frac{1}{N}\sum_{\mathbf{k}} V_{\mathbf{k}}^2\delta(E-E_{\mathbf{k}}). \tag{26}$$

The original *lattice* Green's function is that of the d level. Therefore, solving the problem defined by the impurity Hamiltonian of Eq. (24) for a given G_0 and applying the self-consistency conditions Eqs. (22) and (23) one has the so-called local impurity self-consistent approximation (LISA), which is the exact solution of a $d\rightarrow\infty$ problem. Interestingly enough, the above impurity Hamiltonian has been used in the past to model core-level relaxation in the x-ray problem.[48] However, in the context of the LISA approach, its significance becomes much more general. Just as the repulsive Anderson impurity model for the Hubbard model, it plays the role of a ''paradigm'' impurity model for the physics contained in the Holstein Hamiltonian. Though the advantages of using an impurity parametrization of the $d\rightarrow\infty$ problem have been extensively reported in Ref. 24 (we also refer to the original references), we must stress, as a general fact, that such a parametrization is not unique in the LISA context.

A. The zero-temperature formalism

In the case of one single electron the Green's function at zero temperature in terms of the impurity operators is

$$G(t)=-i\theta(t)\langle 0|d(t)d^{\dagger}(0)|0\rangle. \tag{27}$$

This function describes the propagation amplitude of the impurity electron created from the vacuum at time zero and destroyed at time t. Fourier transforming Eq. (27) leads to the resolvent

$$G(\omega)=\langle 0|d\frac{1}{\omega+i\delta-H}d^{\dagger}|0\rangle, \tag{28}$$

which has the correct prescription $\delta>0$ for convergence of the time integrals. The vacuum energy is defined here to be zero.

Solving the lattice problem requires finding the solution of the impurity problem for any given G_0. Let us separate the

impurity Hamiltonian of Eq. (24) into H_0 and H_I, where H_0 alone leads to the effective free propagator G_0 and H_I is the local interaction term, then an operator identity for the resolvent holds

$$\frac{1}{z-H}=\frac{1}{z-H_0}+\frac{1}{z-H_0}H_I\frac{1}{z-H}. \tag{29}$$

The diagonal matrix element of this operator on the impurity zero-phonon state $d^\dagger|0\rangle$ is the Green's function of Eq. (28). To proceed further one needs to introduce the generalized matrix elements[48]

$$G_{n,m}=\langle 0|\frac{a^n}{\sqrt{n!}}d\frac{1}{\omega+i\delta-H}d^\dagger\frac{(a^\dagger)^m}{\sqrt{m!}}|0\rangle \tag{30}$$

so that the element $G_{0,0}$ will be the solution of the $T=0$ problem.

In the case of H_I given by Eq. (24), to express the matrix element of the right term in Eq. (29) one takes advantage of the linearity of the interaction term in the electron density operator $n=d^\dagger d$. Namely, introducing a set of zero-electron p-phonon states $|0,p\rangle=(a^\dagger)^p/\sqrt{p!}|0\rangle$ one can write

$$H_I=\sum_p d^\dagger|0,p\rangle\langle 0,p|d(a+a^\dagger), \tag{31}$$

leading to the recursion formula for the $G_{n,m}$'s

$$G_{n,m}=G_{0n}\delta_{n,m}-g\sum_p G_{0n}X_{n,p}G_{p,m}, \tag{32}$$

where $G_{0n}=G_0(\omega-n\omega_0)$ is the diagonal element of the free resolvent and $X_{n,p}$ are the phonon displacement matrix elements:

$$X_{n,p}=\sqrt{p+1}\,\delta_{n,p+1}+\sqrt{p}\,\delta_{n,p-1}. \tag{33}$$

Equation (32) is solved in matrix notation:

$$\mathbf{G}^{-1}=\mathbf{G_0}^{-1}+g\mathbf{X}. \tag{34}$$

One immediately recognizes that, due to the particular form of $\mathbf{X}$, $\mathbf{G}^{-1}$ is a tridiagonal matrix, so that the solution of the problem is reduced to the inversion of a matrix in arbitrary dimensions. Following the lines given in Ref. 49 (see alternatively Ref. 48) one can express the diagonal element of the $\mathbf{G}$ matrix in terms of the diagonal and nondiagonal elements of $\mathbf{G}^{-1}$. The local propagator (the 0,0 element of $\mathbf{G}$) is obtained in terms of a continued fraction expansion, as a functional of the ''bare'' propagator G_0:

$$G(\omega)=\cfrac{1}{G_0^{-1}(\omega)-\cfrac{g^2}{G_0^{-1}(\omega-\omega_0)-\cfrac{2g^2}{G_0^{-1}(\omega-2\omega_0)-\cfrac{3g^2}{G_0^{-1}(\omega-3\omega_0)-\cdots}}}}. \tag{35}$$

Due to the impurity analogy, *this is also the local propagator of the original lattice problem*, provided that Eqs. (22) and (23) are fulfilled. As a special case, one notices that in the atomic limit, setting $G_0(\omega)=\omega^{-1}$, Eq. (35) is nothing but an alternative representation of the atomic propagator, Eq. (13). In the general case, the self-energy is immediately recognized as a functional of G_0, from the self-consistency condition (23)

$$\Sigma(\omega)=\cfrac{g^2}{G_0^{-1}(\omega-\omega_0)-\cfrac{2g^2}{G_0^{-1}(\omega-2\omega_0)-\cfrac{3g^2}{G_0^{-1}(\omega-3\omega_0)-\cdots}}}. \tag{36}$$

This allows one to solve the impurity problem in the dynamical mean-field theory. Once the self-energy is obtained for a given G_0, the local lattice propagator is calculated from Eq. (22) and using Eq. (23) a new G_0 is obtained. After few numerical iterations a fixed point G_0^* is reached, and the lattice local propagator $G^{-1}=G_0^{*-1}-\Sigma[G_0^*]$ is determined. We emphasize that Eq. (36) only involves a *discrete* set of values of G_0 and this turns out to be a drastic simplification of the calculation. Moreover, in the Bethe lattice the impurity and the local propagator are simply related:

$$G_0^{-1}(\omega)=\omega-\frac{t^2}{4}G(\omega), \tag{37}$$

which, replacing Eqs. (22) and (23), simplifies the calculation.

Let us now show diagrammatically how formula (36) exactly sums up all of the self-energy contributions. It is indeed possible to relate term by term the expansion of Eq. (36) in powers of g considering G_0 as a parameter in the skeleton

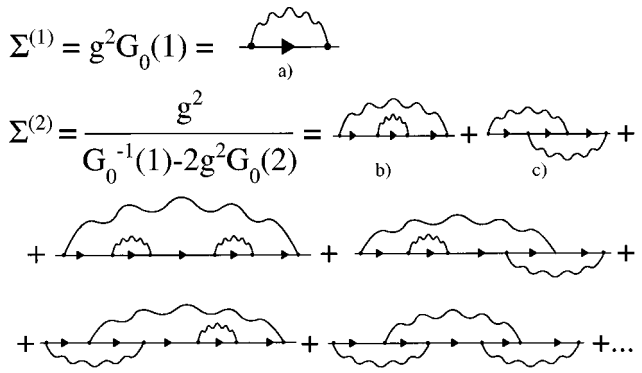

FIG. 2. The CFE expansion diagrams obtained by a truncation of the CFE at the first stage and some of those obtained at the second stage. Diagrams (a), (b), and (c) represent respectively the second and fourth order perturbation theory terms. In this case internal propagators are assumed to be free $\mathcal{G}_0$.

expansion of the self-energy. The relation is obtained through the following steps: (i) first obtain a truncation to a given formal order g^k of the skeleton expansion of the self-energy using the rules previously introduced. (ii) Express the internal *fully interacting* propagator of the skeleton expansion in terms of the ''bare'' impurity propagator G_0 using the self-consistency conditions (22) and (23) and expand the result to g^k. The result is equal to the expansion of the continued fraction to the *formal* order g^k.

It is now instructive to understand the meaning of a finite truncation of the CFE. The self-energy given in Eq. (36) can be defined recursively,

$$\Sigma^{(p-1)}(\omega)=\frac{pg^2}{G_0^{-1}(\omega-p\omega_0)-\Sigma^{(p)}(\omega)}, \tag{38}$$

where p is the stage index of the CFE for Σ. An N-stage truncation of the CFE is defined by neglecting $\Sigma^{(N+1)}$ in Eq. (38). In the resulting diagrammatic expansion *only phonon states* $|n\rangle$ *with* $n \leqslant N$ *appear as intermediate states*. This operates a selection of diagrams, which is different from that based on the perturbative expansion, which by contrast is related to the number of interaction vertices. Indeed, at each step of the truncation an infinite set of diagrams is resummed, *including vertex corrections* (see Fig. 2). As one can easily see by writing the expansion for the atomic limit, the parameter α^2 measures the importance of multiphonon effects and the number of phonons N needed for an accurate description of all the scattering processes should be much larger than α^2. It is interesting to note that a self-consistent noncrossing approximation such as a Migdal scheme, always fails, since it can be put in a CFE context by changing all coefficients of g^n in Eq. (36) to 1.

B. Generalization to a thermalized lattice

The above formalism can be easily generalized to nonzero temperature. The trace performed over free phonon states gives

$$G(\omega)=(1-e^{-\beta\omega_0})\sum_n e^{-\beta n\omega_0}G_{n,n}(\omega), \tag{39}$$

where $G_{n,n}$ are the diagonal elements of the correlation matrix defined in Eq. (30) and calculated by means of the Dyson equation (34).

The calculation of the diagonal elements $G_{n,n}$ follows the lines given in Refs. 49 and 48. The inverse of each $G_{n,n}(\omega)$ is now the sum of an *infinite* continued fraction, which is similar to the result at $T=0$ plus a *finite* fraction, which formally takes into account the absorption processes at negative frequencies. This reads

$$G_{n,n}(\omega)=\frac{1}{G_0^{-1}(\omega)-A-B}, \tag{40}$$

where

$$A=\cfrac{ng^2}{G_0^{-1}(\omega+\omega_0)-\cfrac{(n-1)g^2}{G_0^{-1}(\omega+2\omega_0)-\cfrac{(n-2)g^2}{\ddots-\cfrac{g^2}{G_0^{-1}(\omega+n\omega_0)}}}} \tag{41}$$

and

$$B=\cfrac{(n+1)g^2}{G_0^{-1}(\omega-\omega_0)-\cfrac{(n+2)g^2}{G_0^{-1}(\omega-2\omega_0)-\cfrac{(n+3)g^2}{G_0^{-1}(\omega-3\omega_0)-\cdots}}}. \tag{42}$$

The solution of the problem now follows the same lines as the zero temperature case.

The relation between the CFE expansion and the perturbation theory can be exploited using the simplification that holds in the zero density limit at nonzero temperatures. The rules for constructing a self-energy diagram at nonzero temperature are easily obtained as a generalization of those obtained in Sec. II B. (1) A general self-energy diagram consists of a single electron line emitting and absorbing phonons. (2) The emission (absorption) of a phonon consists in subtracting (adding) a quantum of phonon frequency ω_0 to the energy of the propagating electron line. Associate to each process a factor $1+f_B(\omega_0)$ when subtracting ω_0 and a factor $f_B(\omega_0)$ when adding ω_0 to the electron line.

The introduction of the temperature energy scale T/ω_0 rules the truncation of the series of CFE Eq. (39). For any finite n we also consider, in the practical evaluation of the spectral function, a finite truncation of B of size N. We therefore have a maximum number of phonons $N+n$ in an intermediate virtual state of which N are emitted and n are absorbed from the thermal bath. Therefore the criterion of truncation valid at $T=0$ ($N \gg \alpha^2$) has to be supplemented by the condition $n \gg T/\omega_0$.

C. Limiting cases in the LISA approach

We discuss here some limiting cases based upon the LISA approach and show that the main properties of the finite-dimensional polaron problem are captured by the infinite-

dimensional limit. We also analyze the adiabatic limit, which, when the polaron becomes localized, involves the breaking of translational symmetry and consequently cannot be achieved using the CFE, which assumes this symmetry.

By expanding to second order the LISA self-energy given by Eq. (36) and substituting the free propagator for the self-consistent G_0 we obtain the perturbative relation of Eq. (4). Then from Eq. (5) and using the semielliptical (Bethe lattice) DOS of Eq. (21) one gets the effective mass:

$$\frac{m^*}{m}=1-2\lambda\gamma\left[1-\frac{1+\gamma}{\sqrt{(1+\gamma)^2-1}}\right]. \tag{43}$$

In the low-phonon-frequency regime, this becomes

$$\frac{m^*}{m}=1+\sqrt{2\gamma}\lambda, \tag{44}$$

which shows the same behavior as in a regular three-dimensional case [see Eq. (6)]. In the large phonon frequency regime we obtain the same result as Eq. (7).

The fourth-order term in the self-energy expansion is

$$\Sigma_4(\omega)=2g^4\mathcal{G}_0^2(\omega-\omega_0)\mathcal{G}_0(\omega-2\omega_0). \tag{45}$$

From the previously stated rules, Σ_4 is the sum of two contributions, e.g., a fourth-order noncrossing diagram [Fig. 2(b)] plus a vertex correction [Fig. 2(c)]. In the zero density limit and in infinite dimensions, *the two contributions are exactly equal*. As a consequence, any noncrossing approximation such as the self-consistent approximation of Engelsberg and Schrieffer[39] is not valid here. In fact, this kind of approximation can be justified by the conventional Migdal's argument[50] restated for Einstein phonons.[39] This argument requires the condition $\lambda\omega_0/E_F\ll 1$, where E_F is the Fermi energy,[33] which is trivially invalidated in the zero density limit where $E_F=0$.

Concerning the spectral properties, most of the perturbative considerations of the three-dimensional case (Sec. II) are valid. Due to the fact that the real part of Σ to second order does not diverge, a finite gap arises in the spectral density for sufficiently large values of the phonon frequency $[\gamma>2/(1+2\lambda)]$.

In the atomic limit, all the self-consistent $G_0^{-1}(\omega-n\omega_0)$ in Eq. (35) must be substituted by their atomic value $\omega-n\omega_0$. The resulting continued fraction can be also independently obtained by solving directly the atomic model through the resolvent technique described in the previous section. The advantage of this formulation, compared to the LF result [Eq. (13)] is to yield immediately the self-energy as a functional of the free atomic propagator. The exact result at finite hopping could then be understood as the result of a coherent potential approximation (CPA) procedure. By CPA we mean the self-consistent approximation that amounts to substituting in the CFE form of the atomic self-energy a self-consistent Green's function for the atomic one.[51] It is worth noting that although the ''pole'' and CFE expressions of the atomic propagator are equivalent, they give different results when extended to finite hopping through the CPA. For example, if one extracts the self-energy for the CPA procedure from Eq. (13), one recovers an expression that agrees with the exact results only for large phonon frequencies.

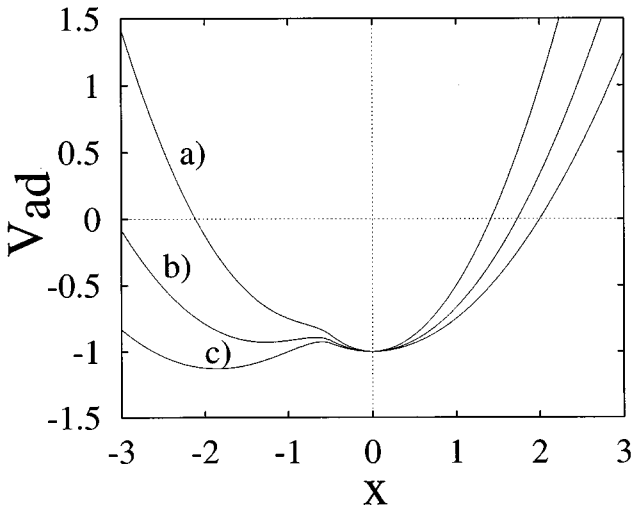

FIG. 3. The adiabatic potential for (a) $\lambda<\lambda_c'$, (b) $\lambda_c'<\lambda<\lambda_c$, and (c) $\lambda>\lambda_c$ (see text).

The Holstein approximation described in Sec. II B can be recovered at low energy by the CFE expansion of the local propagator when ω_0 is the largest energy scale in the self-consistent propagator G_0. In this case, all the $G_0^{-1}(\omega-n\omega_0)$ with $n\geqslant 0$ appearing in Eq. (35) can be replaced by their atomic value, giving an atomic self-energy that yields the exponential renormalization of the effective mass as shown in Sec. III.

Another instructive formula can be derived from the CFE in the limit $\omega_0\to 0$. In this case all the $G_0(\omega-n\omega_0)$ in Eq. (35) can be replaced by $G_0(\omega)$ and one recognizes the continued fraction expansion of the complex error function,[52] which can be expressed in terms of an integral:

$$G(\omega)=\int\frac{dx}{\sqrt{2\pi}}e^{-x^2/2}\frac{1}{G_0(\omega)-gx}. \tag{46}$$

The physical interpretation of this formula is that the electron moves within a field of displacements with a Gaussian distribution. Such a distribution can be understood as the ''classical'' limit of the quantum probability distribution of local lattice displacements when the phonon frequency goes to zero while keeping the elastic energy finite. Let us remark that as long as the hopping self-energy term in Eq. (46) is neglected one recovers a Gaussian DOS as predicted for $\omega_0\to 0$ by the atomic limit.

The adiabatic limit is reached when both ω_0 and g go to zero, keeping λ fixed. In this case the CFE yields the free-electron propagator. The problem is that one needs to consider the possibility of translational symmetry breaking. We have developed an independent scheme presented in the Appendix that allows an exact solution at zero phonon frequency, *keeping* λ *finite*. The ground-state energy is determined by minimizing the total energy with respect to the lattice displacement, described by a classical variable. According to the shape of the total energy curve as a function of the lattice displacement (see Fig. 3) we find three different regimes: (i) $\lambda<\lambda_c'$. The only stable minimum corresponds to

an undistorted lattice (delocalized solution, strictly free electron). (ii) $\lambda_c' < \lambda < \lambda_c$. The delocalized solution is still a stable minimum, but a relative minimum appears in the potential at nonzero lattice deformation, corresponding to a metastable localized solution (small polaron). (iii) $\lambda > \lambda_c$. The stable minimum corresponds to a localized solution, where $\lambda_c' = 0.649, \ldots$ and $\lambda_c = 0.843, \ldots$.

Therefore in the $d \to \infty$ Bethe lattice a first-order localization transition occurs at λ_c from a delocalized free electron to a localized polaron. Moreover, for finite values of the coupling, the localized polaron extends over several lattice shells of neighbors around a given localization site, just as in finite dimensions.[19] All these features are quite similar to those found in regular two-dimensional and three-dimensional cubic lattices.

To summarize the discussion of this section, examination of the various limiting regimes in the special case of an infinite-dimensional Bethe lattice shows the consistency of this limit with a three-dimensional situation. This is true as well in the adiabatic regime as in the perturbative and large phonon frequency regimes (shaded areas in Fig. 1). The dynamical mean-field solution, exact in infinite dimensions and presented in the following section, allows us to complete the phase diagram and can be thought of as a controlled interpolation scheme valid at least qualitatively also in finite dimension $d > 2$.

IV. RESULTS FROM THE DYNAMICAL MEAN-FIELD THEORY

Let us now turn to the self-consistent solution for the infinite-dimensional lattice with a semielliptical density of states, by solving Eqs. (37) and (35). We first discuss the ground-state properties, as deduced from the behavior of $\Sigma(\omega)$ close to the ground-state energy.

A. Ground-state properties

The knowledge of the self-energy and of the Green's function allows access to the ground-state properties: the ground-state energy, which is evaluated by solving Eq. (9); the electron-lattice *local* correlation function defined in Eq. (12), which can be evaluated using the Hellmann-Feynman theorem[53] from the first derivative of the ground-state energy with respect to g; the electron kinetic energy, i.e., the average over the ground state of the hopping term of the Hamiltonian Eq. (1), which, using again the Hellmann-Feynmann theorem, is calculated as a derivative of E_0 with respect to t; the average phonon number in the ground state, which can be obtained as a derivative of the ground-state energy with respect to ω_0.

The ground-state properties are summarized in Figs. 4–8. They illustrate the above relevant quantities as functions of the coupling constant λ for three different values of α^2, 1, 2, and 5. The polaron crossover is seen as a continuous change from weakly dressed to quasilocalized electrons. The crossover almost disappears for $\alpha^2 = 1$, while it becomes sharper for large α^2, approaching the first-order localization transition observed in the adiabatic limit $\omega_0 = 0$ (see Appendix). The existence of a smooth crossover rather than an abrupt transition (for finite ω_0) corroborates the general proof previously derived by Gerlach and Löwen.[54] However, the ground-state properties are quantitatively calculated here for any value of the parameters.

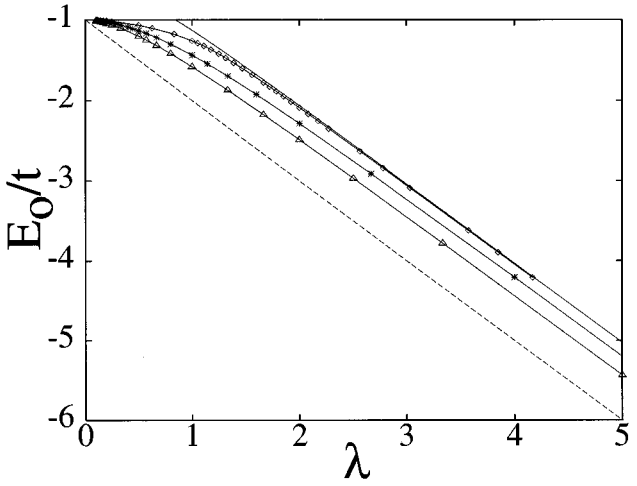

FIG. 4. Ground-state energy vs λ for three different values of the parameter $\alpha^2 = 1,2,5$ (triangles, asterisks, diamonds). Continuous line is the adiabatic limit; the dashed line is the strong coupling result.

Let us discuss these results in more detail. Concerning the ground-state energy depicted in Fig. 4 one sees that it is bounded from above by the adiabatic result ($\omega_0 = 0, \alpha^2 \to \infty$) and from below by the large-phonon frequency result ($\omega_0 = \infty, \alpha^2 = 0, E_0 = -\lambda$). As the coupling increases, the crossover occurs for λ of the order of λ_c, where λ_c is the critical coupling strength obtained in the adiabatic limit. The behavior of the effective mass is shown in Fig. 5. For large λ it increases with α^2, but remains smaller than Holstein's prediction of Eq. (17), which is attained asymptotically only for very large couplings.[55]

Notice also that for $\alpha^2 = 1$ we do not observe any change in the curvature of the effective mass, showing that no appreciable crossover occurs but rather a smooth increase of the effective mass from 1 towards $\exp(1) \sim 2.7$. On the other

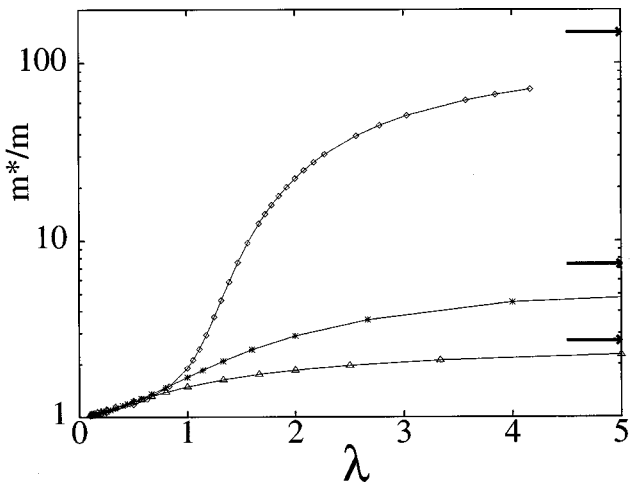

FIG. 5. Polaron effective mass in units of the bare electron mass vs λ for three different values of the parameter $\alpha^2 = 1,2,5$ (triangles, asterisks, diamonds). Arrows mark the Holstein's approximation result $\exp(\alpha^2)$.

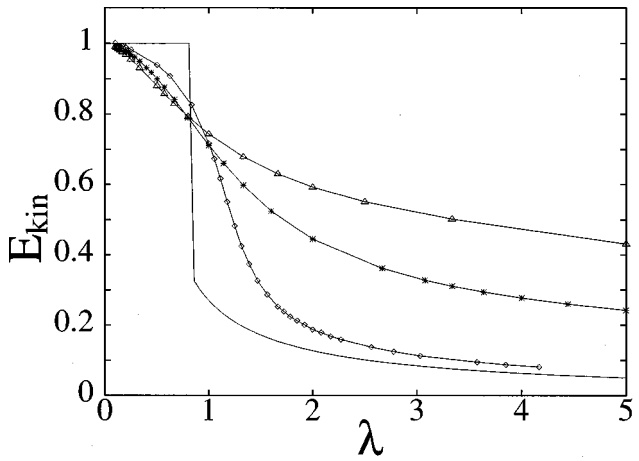

FIG. 6. Polaron kinetic energy vs λ for three different values of the parameter $\alpha^2=1,2,5$ (triangles, asterisks, diamonds). Continuous line is the adiabatic limit result.

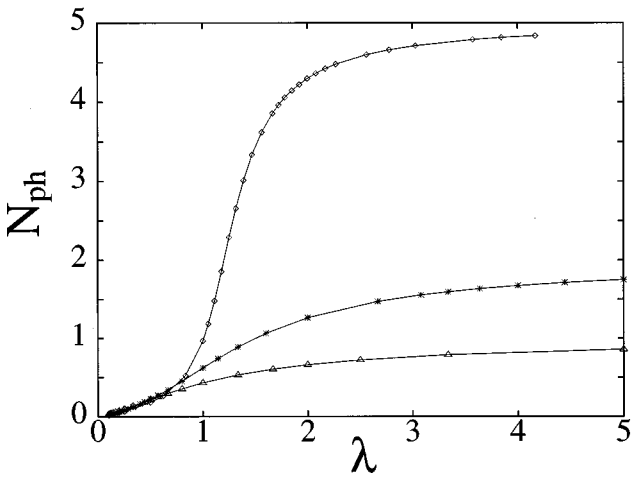

FIG. 8. Average number of phonons in the ground state vs λ for three different values of the parameter $\alpha^2=1,2,5$ (triangles, asterisks, diamonds). Arrows mark the strong coupling result α^2.

hand, one notices that for $\lambda<\lambda_c$, the effective mass diminishes as α^2 increases, in agreement with the adiabatic ($\alpha^2\to\infty$) prediction of having unrenormalized electrons for small couplings. Therefore, the mass renormalization as a function of α^2 behaves in opposite ways for $\lambda<\lambda_c$ and $\lambda>\lambda_c$. For infinite α^2 ($\omega_0=0$), m^*/m jumps from 1 to ∞.

The spectral properties, discussed in the next paragraph, will clarify this singular behavior, which indeed reflects the breakdown of the perturbation theory for $\lambda>\lambda_c$.

The ground-state kinetic energy is shown in Fig. 6. Again a crossover is found as a change of curvature only for $\alpha^2>1$ and becomes sharper as the adiabatic limit is approached. Figure 7 displays the electron-phonon correlation function (i.e., the local deformation of the lattice). To make a comparison with the well-defined adiabatic limit, it is convenient to scale this quantity by the strong coupling value 2α. A sharp crossover towards large electron-lattice local correlations is found for large α^2. Similarly, the number of phonons in the ground state, shown in Fig. 8 attains the value

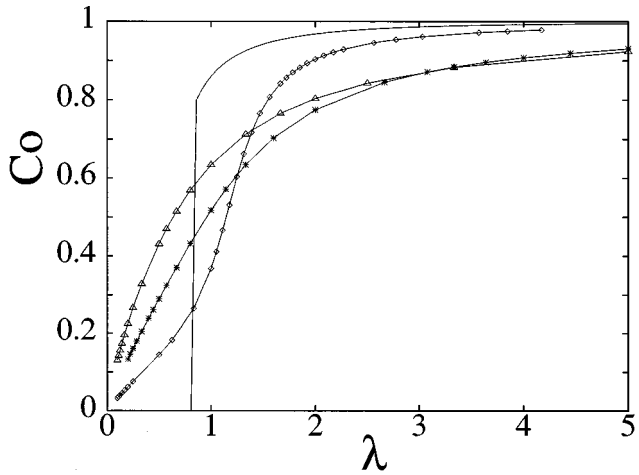

FIG. 7. Electron-phonon local correlation function scaled with the strong coupling result 2α vs λ for three different values of the parameter $\alpha^2=1,2,5$ (triangles, asterisks, diamonds). Continuous line is the adiabatic limit result.

α^2 only asymptotically for very large coupling. As a general property, one must stress that the Holstein values for all the above quantities are obtained assuming a *local* lattice deformation. The gradual behavior we find towards these values is due to the finite extension of the polaron, i.e., of the electron wave function and lattice deformation over several shells of lattice neighbors. This is also true in the $d\to\infty$ limit, and in particular causes the kinetic energy to be nonzero, even in the adiabatic limit for $\lambda>\lambda_c$ (see Appendix).

Recently, a numerical study[34] by diagonalization on small clusters has led to the conclusion that the polaron crossover occurs when both conditions $\alpha^2>1$ and $\lambda>1$ are fulfilled. According to this interpretation, to have a polaron one requires that $\lambda>1$ for $\gamma<1$ or $\alpha^2>1$ for $\gamma>1$. CFE results are in qualitative agreement with this statement since we observe no appreciable crossover for any value of λ provided $\alpha^2<1$, and in the opposite case the crossover is found at around $\lambda\sim1$ and becomes sharper as α^2 is increased. A better understanding of this behavior can be gained by plotting the effective mass in the whole parameter space (γ, λ), Fig. 9(a). The isolines corresponding to large effective mass define the polaron region. We see that for large λ and γ the effective mass depends only on α^2 as predicted by the strong coupling theory. As γ decreases, the crossover gets sharper until it becomes a real first-order localization transition for $\gamma=0$ at the adiabatic critical value λ_c. Finally it must be remarked that all these results are in qualitative agreement with Monte Carlo simulations,[20,32] which show that *at finite phonon frequency* the ground-state properties in the polaron crossover are not very dependent on the dimensionality.

B. Spectral properties at $T=0$

As in other strong coupling problems such as the Hubbard model, the standard mean-field or variational techniques (based here on the Lang-Firsov approximation followed by phonon averaging) do not allow one to go beyond the low-energy properties. Instead, the dynamical mean-field theory provides a way to explore the whole electron spectrum.

The spectral properties are directly extracted from the knowledge of the local propagator, and reflect the structure

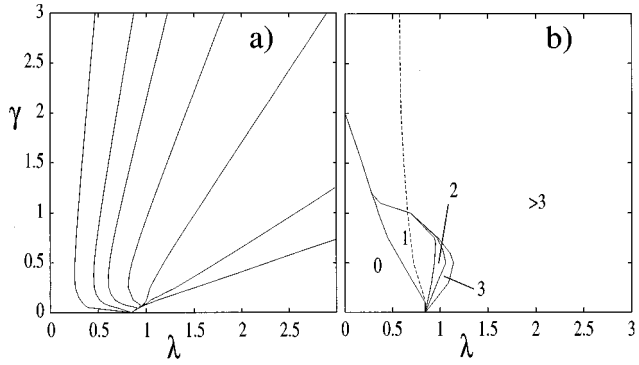

FIG. 9. Both ground-state and spectral properties are summarized in the λ,γ plane. (a) Effective mass isolines (from left to right $m^*=1.1,1.2,1.3,1.5,2,5,20$). In this picture a curve with constant α^2 is a straight line starting at the origin (see also Fig. 1). (b) The number of gaps in the electron spectral density. Near the adiabatic limit all the lines that separate regions of equal number of gaps collapse to λ_c. On the right of the dashed line at least one point in which the self-energy diverges appears.

of the excited states. Formulas (8) and (9), valid in the case of a local self-energy, obviously apply in the case of the dynamical mean-field theory.

We focus here on the behavior of the spectral density and of the self-energy. In particular, a nonzero $\mathrm{Im}\Sigma$ reveals an incoherent scattering due to emission and absorption of phonons. More precisely, given a band in $\mathcal{N}(\omega)$ of reduced width t^* we can determine if an excitation at a given frequency has a coherent or an incoherent character. To do this we expand the spectral function around the peak located at $\omega^*-\mathrm{Re}\Sigma(\omega^*)=\epsilon$. This relation defines a pole $\omega^*(\epsilon)$, which, in the case of a translationally invariant lattice, gives the band dispersion. Then assuming around the pole ω^* an effective mass inversely proportional to the effective bandwidth and using Eq. (5) with $E_0\rightarrow\omega^*$ we get approximately $\omega-\epsilon-\mathrm{Re}\Sigma(\omega)\simeq(t/t^*)(\omega-\omega^*)$ and

$$A(\epsilon,\omega)\simeq-\frac{1}{\pi}\frac{t^*}{t}\frac{\Gamma}{(\omega-\omega^*)^2+\Gamma^2}, \tag{47}$$

where $\Gamma=-(t^*/t)\mathrm{Im}\Sigma(\omega^*)$. Then the excitation is coherent if its lifetime $(1/\Gamma)$ is much greater than the characteristic time of the (renormalized) hopping processes $1/t^*$, i.e., $\Gamma\ll t^*$. This gives the coherence condition $\mathrm{Im}\Sigma(\omega^*)\ll t$ (and

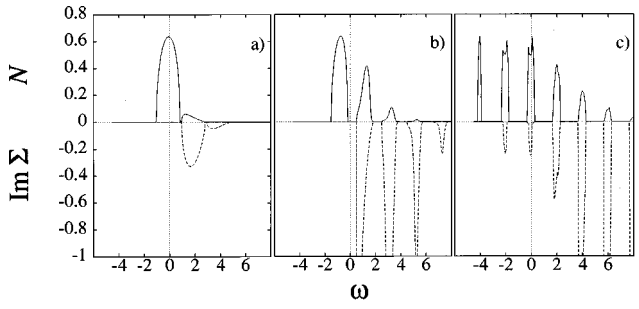

FIG. 10. Spectral density (continuous line) and imaginary part of the self-energy (dashed line) in the large phonon frequency regime $\gamma=2$, for $\lambda=$(a) 0.08, (b) 0.75, and (c) 4.0. In this and the following spectra the energies are expressed in units of t.

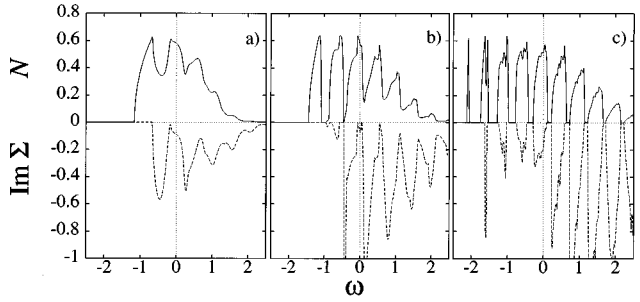

FIG. 11. Spectral density (continuous line) and imaginary part of the self-energy (dashed line) in the intermediate phonon frequency regime $\gamma=0.5$, for $\lambda=$(a) 0.4, (b) 1.0, and (c) 2.0.

not t^*). If the coherence condition holds, the quasiparticle pole $\omega^*(\epsilon)$ is well defined since the spectral function has a sharply defined peak at $\omega=\omega^*(\epsilon)$ with a width much less than the renormalized bandwidth.

The scenario for polaron formation can be analyzed from Figs. 10–12 where the spectral density and the imaginary part of the self-energy are shown in the large-, intermediate-, and low phonon frequency regimes, respectively, for increasing values of λ. Generally speaking, in all regions of parameters, the condition to form a (quasi)particle of large effective mass such as a small polaron is that *a narrow coherent band emerges at low frequency*. We call it the zero-phonon *polaronic band*. It is worth noticing that when a polaron with a large effective mass is formed one always observes several bands in the spectra, and the one at lowest energy is *perfectly coherent* $(\mathrm{Im}\Sigma=0)$, since this band lies entirely below the minimum energy $E_0+\omega_0$ for inelastic scattering.[39] Though this feature is common to the spectra in all parameters regions, the way in which polaronic behavior is exhibited in the spectral properties is very different according to the value of the adiabatic ratio γ.

Let us first discuss the large-phonon frequency regime. In this case (see Fig. 10) the formation of the polaron from the point of view of the spectral properties is a smooth crossover. For $\gamma>2$, the spectra always display a multipeaked structure [see also Fig. 9(b)] in which the $n=0$ polaron band and the edges of the first excited bands are perfectly coherent. These structures are subbands corresponding to polaron states with n phonons excited, and can be easily understood by switching on the hopping term from the atomic limit. For

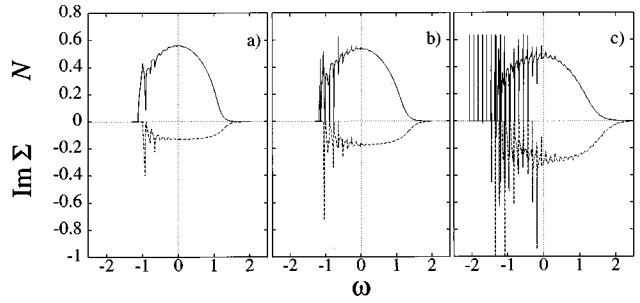

FIG. 12. Spectral density (continuous line) and imaginary part of the self-energy (dashed line) in the low phonon frequency regime $\gamma=0.125$, for $\lambda=$(a) 0.7, (b) 1.0, and (c) 2.0. The δ-like divergencies of the self-energy near the first four tiny bands are not reported in this figure (see Fig. 13).

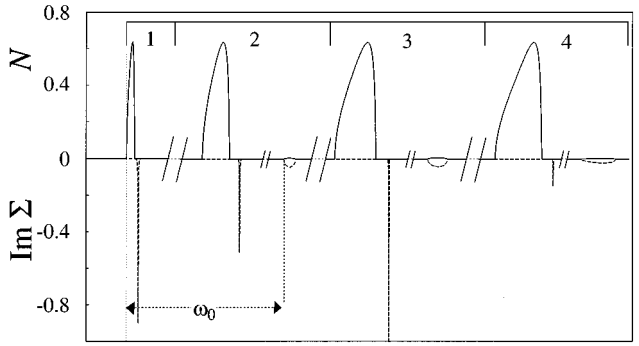

FIG. 13. Spectral density and ImΣ with the parameters of Fig. 12. The low-energy part of the spectrum is shown, illustrating the nth substructures with $n=1,\ldots,4$ $(0,\ldots,3$ excited phonons). For each given $n\geqslant 1$, the coherent and incoherent states are separated by a gap. The δ peaks in ImΣ are revealed by adding a small imaginary part to the frequency ω. The width of each structure has been reported using different scales to compare the shape of each peak. The bandwidths of the four coherent peaks are respectively from left to right: 7.2×10^{-7}, 9.8×10^{-6}, 8.33×10^{-5}, and 5.0134×10^{-4}. The widths of the incoherent structures are from left to right 6.1×10^{-7}, 9.67×10^{-6}, and 8.323×10^{-5}.

very large γ, all the subbands tend to have the same width, in agreement with the predictions from Holstein's approximation;[13] see Eq. (16). For intermediate values of γ, increasing λ causes the shrinking of the width of the low-energy bands and decreases their spectral weight, while higher-frequency bands become more important. The crossover occurs for $\lambda\sim\gamma$ $(\alpha^2\sim1)$ [cf. Fig. 12(c) in which $\alpha^2=2$]. One notices that the envelope of the peaks in the imaginary part of the self-energy tends to reproduce the envelope of the bands in the spectral density, shifted by ω_0, as can be deduced from the CFE. Thus, for $\alpha^2>1$, both the weight and the damping of the subbands tend to increase with their index and then decrease following a roughly Poissonian envelope, with a maximum at $\omega\sim\alpha^2\omega_0+E_p\simeq0$.

Let us now turn to the low phonon frequency regime, in which the formation of polaronic bands is qualitatively different and exhibits novel features. From Fig. 12 we see that a polaronic band emerges from an *incoherent* band around $\lambda\simeq1$. Increasing the value of the coupling, more and more bands emerge, having very small bandwidth. Notice that the low-energy structures are not resolved on the scale of Fig. 12(c), but they can in fact be accurately calculated by the CFE and are shown in detail in Fig. 13. As we shall see below, the relative distance between polaron subbands is expected to be less than ω_0, due to lattice displacements effects. The inverse lifetime ImΣ, on the opposite, reproduces the pattern of the polaron subbands at energies shifted by ω_0. Therefore, if the bandwidth renormalization is strong enough, each nth-order excited band splits further into a doublet of bands separated by a gap, where the main one is coherent and the secondary one is incoherent. The coherent subbands turn out to have equivalent heights and can be interpreted as coherent quantum tunneling out of a distorted lattice site: they correspond to *coherent polaron* bands with $n=0,1,\ldots$ excited phonons.

A qualitative understanding of the low- and high-energy excitations at small γ can be deduced from a comparison with the adiabatic limit results (Appendix). Figure 14 shows

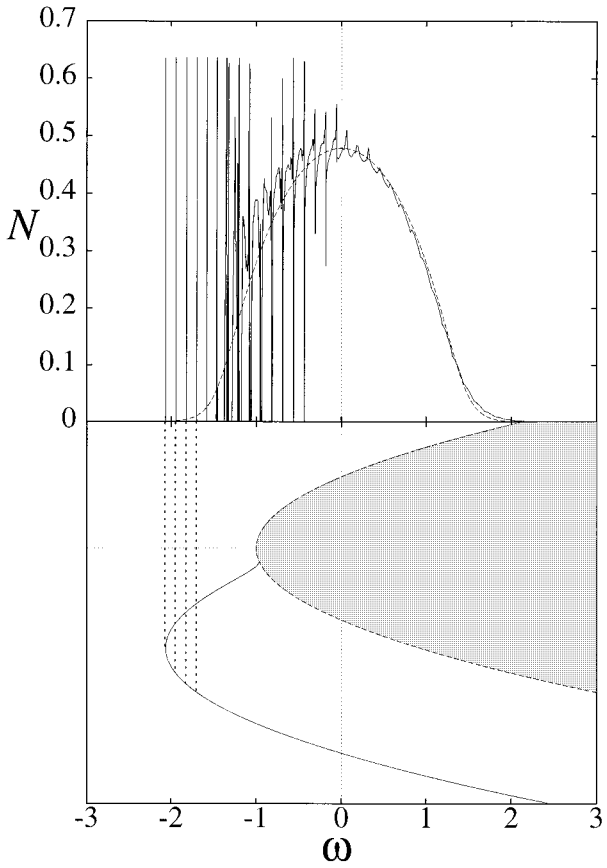

FIG. 14. In the upper panel is shown the spectral density (continuous line) near the adiabatic limit $(\lambda=2,\gamma=0.125)$ compared with the adiabatic strong coupling result (dashed line). In the lower panel the continuous line is the ground-state adiabatic total energy as a function of the lattice displacement (see Fig. 3), the dashed line represents the lowest excited adiabatic level, which is at the bottom of a continuum (shaded area). The zero-point energy is omitted here. See also the Appendix.

the spectrum of Fig. 12(c), in correspondence with the adiabatic potential relative to the same value of the coupling λ. It is clear from Fig. 14 that a low-energy scale can be defined as the region where the spectrum consists of separated subbands. The separation of energy scales can be understood by considering the effect of finite phonon frequency, i.e., by considering quantum corrections to the classical lattice approximation. This yields a series of low-energy bands that are roughly centered around the position of the quantized levels of the ground-state adiabatic potential $V_{\rm ad}^{(b)}(X)$ given in Eqs. (A11) and (A12) and Fig. 14. As the energy is increased from E_0, hese levels become more and more hybridized with the excited adiabatic continuum associated to the undistorted lattice starting at $V_{\rm ad}^{(a)}(0)=-t$. In the real spectrum, one actually observes that the very narrow bands merge into a broad structure just around this energy level, thus defining the amplitude of the low-energy region as $|E_0|-t$. One can also evaluate from the data shown in Figs. 12(c), 13, and 14 a small negative deviation of about 2% of the first band spacings from ω_0, and in general the first four narrow bands in the figure are not exactly equally spaced. This can be explained in terms of the adiabatic potential picture by noticing that the curvature of the total adiabatic

energy near the distorted minima is smaller than near the undistorted position. In fact, a prediction based upon linearization of the adiabatic potential yields a 1.65% deviation from ω_0 for the distance of the first excited level from the ground state of the adiabatic potential.

The nature of the high-energy part of the spectrum is explained using a strong coupling adiabatic approximation, namely the $\omega \to 0$ limit of the CFE (Ref. 56) [see Eq. (46)]. This approximation describes the broad structure as an envelope of resonances separated by a vanishingly small ω_0. The resulting spectrum is shown in Fig. 14 (upper panel) and fits very well the high-energy part of the spectral density. This fit deteriorates at intermediate energies where spiky structures appear, due to the effect of a finite ω_0. The self-energy obtained from Eq. (46) indicates that all the states at intermediate and high energies have an incoherent character.

In the intermediate frequency regime, the structure of the low-energy bands when these are well separated is curious and follows some rules that can be deduced directly from the CFE expansion [see Fig. 11(d)]: the lowest-energy band is always coherent ($\mathrm{Im}\Sigma = 0$) and its shape resembles the original semielliptical unrenormalized DOS even if some asymmetry is observed towards its upper edge. This is not obtained by the usual (Holstein) strong coupling approximation, and could be depicted by a much larger effective mass at the top band edge. On the other hand, the higher-order bands acquire a complexity that can be labeled by the number of ''substructures'' that can be recognized in the band shape and that increases with increasing energy. Moreover, by comparison of Figs. 12 and 11 we see that the transition with increasing λ from a single band structure to a multipeaked structure at low frequencies is much more abrupt for small than for intermediate γ, and in the former case it turns out to occur around the adiabatic critical value of the coupling λ_c.

Let us now focus in more detail on the mechanism for gap opening in the low and intermediate phonon frequency regimes ($\gamma < 2$). The number of well-separated subbands is shown in Fig. 9(b) as a function of the parameters λ and γ. One notices that there is a large region of the parameters space in which the spectral density consists of only two structures: a single coherent polaronic band and a high-energy band, which is mostly incoherent. In this region, approximation (16), which, apart from the low-energy coherent peak, displays an incoherent spectrum made of separated subbands, is not correct. The extent of this region reduces as the adiabatic ratio is reduced and for very low phonon frequency the system undergoes a rapid crossover to a multipeaked structure at around λ_c. The emergence of a coherent band, separated by a finite energy gap from the continuum can be seen as λ increases on Fig. 15. As a critical value of λ is approached, a pseudogap appears together with a large damping of the states in the same energy range. At higher λ, the gap is formed and keeps increasing until a second gap is formed at higher energy, and so on. By the way, let us underline that the total spectral weight carried by the polaron bands, when they are well separated, is in general different from that obtained in the atomic limit. For instance, the $n=0$ band spectral weight is always larger than $e^{-\alpha^2}$.

An effect related to the formation of subbands, which arises in the intermediate coupling regime, is the divergency

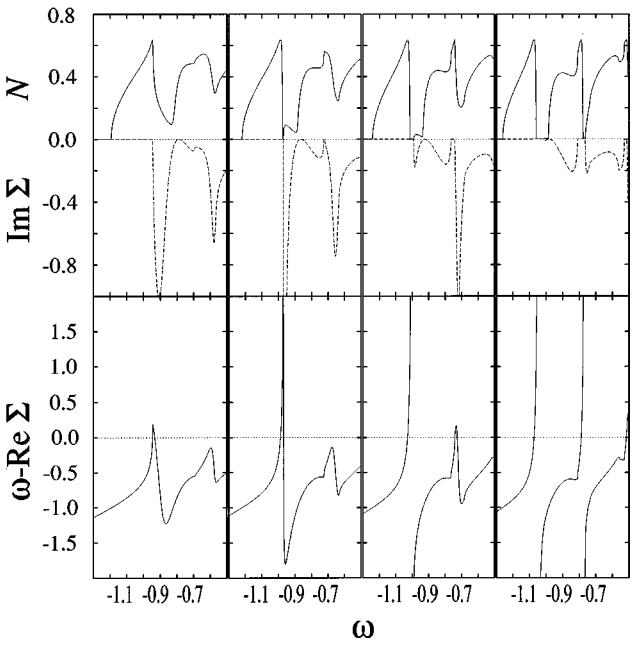

FIG. 15. Evolution of the spectral density and imaginary part of the self-energy at low energy for growing λ (upper panel) for $\gamma = 0.25$ and, from left to right: $\lambda = 0.7, 0.78, 0.84, 0.9$. The lower panel shows $\omega - \mathrm{Re}\Sigma$.

of the self-energy at one and subsequently more frequencies located in the gaps as the coupling strength is increased. In the presence of disorder, external excitations, or at finite temperature, a nonzero spectral density can appear around these energies. We thus expect such excited states within the gaps to have a huge damping and to be localized, while the ground state can keep its delocalized character. For that motivation the authors[35] who found such behavior in the context of the Holstein-Hubbard model named it *dynamical localization*. We must stress that the relevance of such a phenomenon concerning the mobility properties such as the ac conductivity cannot be tested using the CFE formalism. However, we draw attention to the fact that this is a very general phenomenon, which occurs here for a single electron as a polaronic feature; i.e., is related to the multipeaked structure of the Green's function.

The occurrence of such self-energy divergencies requires that the states at the edges of two consecutive bands have an infinite lifetime ($\mathrm{Im}\Sigma = 0$) at zero temperature. In this case, the self-energy fulfills the Eq. (9) at the extrema of the energy gap, so that the real part of $\omega - \Sigma$ changes sign within the gap without crossing the values $\pm t$. As a consequence a divergency in $\mathrm{Re}\Sigma$ occurs at a point ω_L located in the gap. In the Bethe lattice we have the condition

$$\omega_L - \frac{t^2}{4} G(\omega_L - \omega_0) - \Sigma^{(2)}(\omega_L) = 0, \tag{48}$$

where $\Sigma^{(2)}(\omega_L)$ is the second stage expansion of the self-energy in the CFE of Eq. (38). Equation (48) may have more than one solution; i.e., many such points are expected for large values of λ (see Fig. 13). In the atomic limit ($\lambda \to \infty$) there is an infinite number of them, located in the gaps between the peaks of the atomic spectral density.

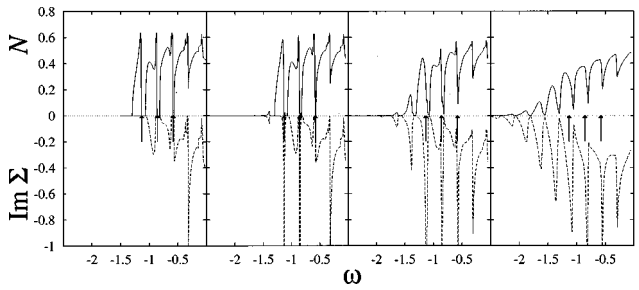

FIG. 16. Evolution of the low-energy spectral density and imaginary part of self-energy with temperature in the intermediate regime $\gamma=0.25$ and $\lambda=1.0$. From left to right $T=0,0.2,0.4,0.8$. Arrows mark points in which the self-energy diverges at $T=0$.

In the (λ,γ) plane, at least one self-energy divergency exists on the right of the dashed line in Fig. 9(b). We note that a self-energy divergency is formed only in a preexisting energy gap. Accordingly, when increasing the coupling strength a gap appears first, separating a coherent polaronic peak from an incoherent excited band, and then a self-energy divergency occurs in the gap when the states at the bottom of the excited band become coherent.

This phenomenon should affect the spectral properties in the presence of disorder[35] or at finite temperatures (see below). In fact, whenever there is a mechanism that is able to give rise to excited states in the proximity of those special points (this can be due to the Lorentzian tails induced by disorder) the singularity in the imaginary part of the self-energy becomes a finite broadening Lorentzian, which implies a loss of coherence of the neighboring states. The consequences on the electronic spectra at finite temperatures will be analyzed in the following section.

C. Spectral properties at finite temperatures

In this section we present the results obtained at finite temperature using the CFE formulation of Eq. (39) and following. The analysis focuses on the intermediate regime where no ''classical'' schemes of approximation are available.

In Holstein's original treatment of polaron motion,[2,37] a distinction is made between transition amplitudes that are *diagonal* in the phonon number, contributing to the polaron coherent motion around the ground-state energy, and those that are *nondiagonal*, giving rise to hoppinglike motion. While the former decrease in the presence of thermal disorder, the latter are thermally activated. This allows one to determine a crossover temperature $T\sim 0.4\omega_0$ where the polaron crosses over from coherent to hopping like motion, which is believed to hold at strong coupling or in the large-phonon frequency regime.

This crossover can also be observed in the one-electron Green's function. To this purpose, we show the spectra in the intermediate coupling regime for increasing T (see Fig. 16). The effect is twofold: first, as is already known from the atomic limit[37] [see Eq. (20)], polaron peaks appear at negative energies. Secondly, scattering by thermally populated phonon states causes finite lifetime effects, in addition to the zero-temperature scattering processes (see Sec. IV B), as can be seen by inspecting the imaginary part of the self-energy. Indeed, one notices that the negative-n subbands are incoherent. Moreover, at low T, a small peak appears in $\mathrm{Im}\Sigma$, close to the upper boundary of the $n=0$ polaron band. For larger T, some spectral weight develops in this region and contributes to gradually broaden this band, until the gap eventually disappears. *This effect is enhanced in the vicinity of a self-energy divergency*, which is extremely sensitive to thermal disorder. This gives rise to an inhomogeneous broadening of the main polaron band.

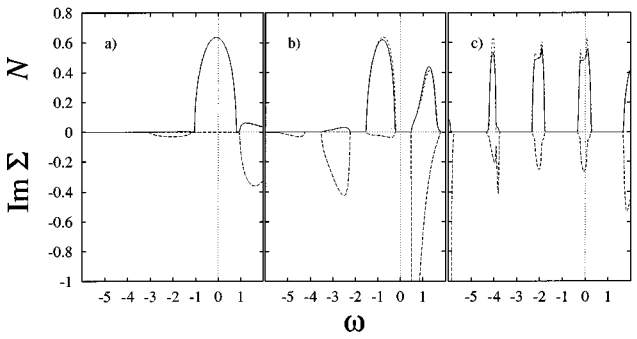

FIG. 17. Spectral density (continuous line) and imaginary part of self-energy (long dashed line) for $\gamma=2$ at $T=0.4$. The spectral density at $T=0$ is shown for comparison (short dashed line). Panels (a)–(c) refer to the same λ's as Fig. 10.

By evaluating the number of coherent states (with $\mathrm{Im}\Sigma\ll t$) within the low-energy subbands in the intermediate coupling regime, one can qualitatively confirm the validity of Holstein's prediction for the crossover temperature, i.e., $T\sim 0.3-0.4\omega_0$. On the other hand, the high-energy part of the spectra is slightly smoothed by the temperature.

A different scenario holds for other values of the parameters. Results are presented in Figs. 17–19 where the low-energy part of the electronic spectra is shown for the same parameter values as in Figs. 10–12, for $T=0.4\omega_0$. One notices that in the high phonon frequency regime, the gaps between polaron bands exist even at high temperatures, and temperature weakly affects the overall shape of the positive nth order polaron subbands (see Fig. 17). On the contrary, for low phonon frequencies, the shape of the polaron subbands is drastically modified (see Fig. 19): the spectral weight of each of them is roughly conserved (for not too large T), but they are noticeably enlarged, and consequently their height diminishes. One must underline that at those temperatures the gaps are not destroyed by thermal fluctuations, apart from vanishingly small spectral density tails.

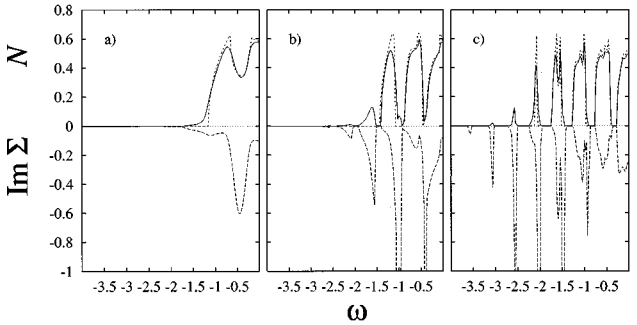

FIG. 18. Spectral density (continuous line) and imaginary part of self-energy (long dashed line) for $\gamma=0.5$ at $T=0.4$. The spectral density at $T=0$ is shown for comparison (short dashed line). Panels (a)–(c) refer to the same λ's as Fig. 11.

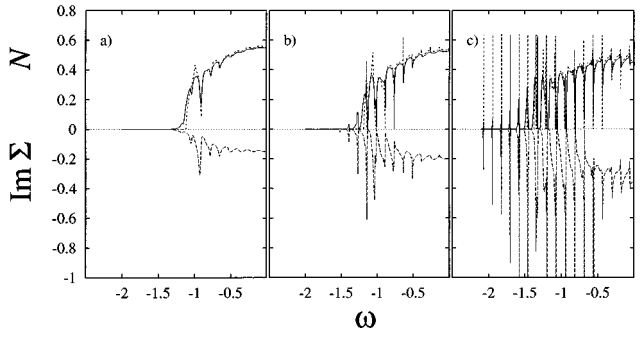

FIG. 19. Spectral density (continuous line) and imaginary part of self-energy (long dashed line) for $\gamma=0.125$ at $T=0.4$. The spectral density at $T=0$ is shown for comparison (short dashed line). Panels (a)–(c) refer to the same λ's as Fig. 12.

V. CONCLUSION

We have shown how the dynamical mean-field theory can be successfully used to solve the single polaron problem at any temperature. The form of the propagator as a continued fraction expansion, together with the self-consistency condition for the noninteracting local impurity propagator, shows that this theory yields an *analytic* solution of the problem, even if some elementary numerics is required to obtain the full spectrum. We have also presented in Sec. II some results in the limiting regimes in the infinite-dimensional case in order to show that the use of a semielliptic free DOS gives sensible results, in agreement with the usual three-dimensional solutions. This gives confidence that the results from the dynamical mean-field theory quite reliably reflect the actual physics in dimension larger than two. On the contrary, in the one-dimensional case, one or more gaps are always present in the spectrum; i.e., polarons form at any coupling.[33]

The properties we find for the ground state are in agreement with the conventional wisdom, in particular the absence of a phase transition, as soon as quantum fluctuations of the lattice are taken into account. The crossover gets sharper as the phonon frequency is decreased for fixed λ, and becomes an abrupt transition from a free electron state to a localized small polaron state at $\gamma=0$. This comes directly from the first-order nature of the transition in the adiabatic limit, clearly displayed by the direct solution.

Beyond the ground-state properties, the full electronic spectrum clarifies the nature of the polaron crossover. For low and intermediate phonon frequencies, as the coupling is increased, several energy gaps successively open up in the spectrum, leaving at low energies coherent or quasicoherent polaronic subbands. These bands can be followed up to very large couplings or large phonon frequencies towards the atomic limit. Therefore they are the manifestation of nonperturbative processes, as is clearly demonstrated by the interpretation of the CFE in terms of a diagrammatic expansion. Thus, even if the ground-state properties show a continuous crossover, some higher-energy features show a qualitative change of behavior, the phenomenon of gap opening.

Let us make more precise the ''lattice'' interpretation of these polaronic subbands. Once the self-energy $\Sigma(\omega)$ is known, and for a given noninteracting lattice DOS, an effective dispersion relation can be found for each well-separated subband, by finding the poles of the spectral function Eq. (8). This corresponds to what is commonly understood as polaron states, i.e., bound states of an electron with a phonon cloud, a number n of phonons being excited in addition. For a translationally invariant finite-dimensional lattice the quantum numbers underlying the local (integrated) spectral function are the *total* momentum K of the polaron[18] and the excited phonon number n. This obviously holds only if the subbands are coherent, i.e., only for low enough n, according to the values of λ and γ.

The low phonon frequency regime exhibits in the crossover region a coexistence of extremely narrow polaronic subbands at low energy and a broad featureless continuum at high energy. While the low-energy features directly follow from the atomic or high phonon frequency limit, the continuum is directly related to the adiabatic solution. The behavior near the critical point $(\lambda=\lambda_c,\gamma=0)$ can be understood as follows: increasing γ, the discontinuity in the low-energy properties becomes a sharp crossover, due to very weak coherent tunneling between small polaron states and quasifree states of the equivalent impurity model. Translated into the language of the lattice problem, it leads to the emergence of coherent ''heavy'' polaron quasiparticle states (''resonances''). However, the high-energy part of the spectrum does not reveal any qualitative change in this region of parameters.

This behavior demonstrates how the usual concept of ''adiabaticity,'' as commonly employed in metals for small ω_0, fails in the present problem: the sharp transition at λ_c and the occurrence of extremely narrow polaron features indicates on the contrary the occurrence of an ''adiabaticity catastrophe.'' This is due to the relevance of high-order vertex corrections in the perturbation expansion.

In this work the application of the LISA approach has been limited to the one-particle propagator. In fact, no exact procedure has been found yet to calculate analytically, for instance, two particle propagators, which would allow one to compute the (dc and optical) conductivity of polarons. Although at zero density it is impossible to access the correlation functions involved in the calculation of the optical conductivity, let us mention that our results suggest an interpretation of the infrared response of oxide superconductors in the insulating phase. In these materials,[9] absorption spectra for low carrier densities exhibit a discrete set of narrow peaks at low energies plus an incoherent background at higher energies. From our point of view, this could be ascribed to multiphonon excitations in the intermediate phonon frequency regime. On the other hand, a better understanding of the polaron crossover could be gained by calculating the dynamical electron-lattice correlation function.[57]

Let us finally comment on future extensions of this technique to finite electron densities. As mentioned before, the CFE expansion keeps for the self-energy the same functional structure as that of the atomic limit. Thus it is equivalent to a CPA approach, which could be extended at finite densities. It is, however, easy to show (by perturbation expansion) that the CPA approximation fails even at the first nonvanishing order in the density. As far as spectral properties are concerned, the CPA failure is particularly evident in the low-energy part of the spectrum, as is well known from equivalent approximations for the Hubbard model. Nevertheless,

our main result, i.e., the coexistence of low-energy coherent and high-energy incoherent structures is a picture that should be qualitatively preserved at least at low carrier densities.

ACKNOWLEDGMENTS

S.C. acknowledges financial support from Université Joseph Fourier, Grenoble and hospitality of Laboratoire d'Etudes des Propriétés Electroniques des Solides. We are grateful to S. Caprara, C. Castellani, A. Georges, M. Grilli, F. Marsiglio, and J. Ranninger for stimulating discussions or comments. CNRS-LEPES is associated with Université Joseph Fourier, Grenoble.

APPENDIX: THE ADIABATIC SOLUTION

In this appendix we will solve the problem of one electron moving in an infinite coordination *static* Bethe lattice. To introduce the adiabatic limit (static lattice) one notices that the free Einstein phonon Hamiltonian can be written as

$$H_{\rm ph}=\sum_i \frac{P_i^2}{2M}+\frac{1}{2}M\omega_0^2 X_i, \tag{A1}$$

where P_i are the impulses, X_i are the coordinates of the ionic motion, M is the ionic mass, and ω_0 the frequency of each oscillator. The adiabatic limit is achieved as $M\to\infty$ *keeping* $k=M\omega_0^2$ *constant*.

The electron-phonon interaction can be written as

$$H_{\rm ph}=-g'\sum_i n_i X_i, \tag{A2}$$

where the coupling constant of Hamiltonian Eq. (1) is given in terms of g' by $g=g'/\sqrt{2M\omega_0}$. The polaron energy $\epsilon_p=-g^2/\omega_0=-g'^2/2k$ is then a well-defined quantity in the adiabatic limit.

To perform an adiabatic calculation we have to perform the following steps: (i) calculate the electronic energy for a given set of ionic deformations X_i, (ii) minimize the *total* energy, i.e., electronic energy *plus* lattice elastic energy with respect to the parameters X_i.

An essential relation that is useful in the adiabatic limit comes from the application of the Hellmann-Feynman theorem to the ground state of the static lattice. By deriving the ground-state energy of the Holstein model with respect to the lattice deformation X_i one obtains

$$X_i=\frac{g'}{M\omega_0^2}\langle n_i\rangle. \tag{A3}$$

From this relation it follows that in the case of a single electron, due to charge conservation, only two situations are possible: (a) delocalized solution with $X_i=0$ everywhere since the total charge density per site is zero in the thermodynamic limit, (b) localized solution with some finite $X_i\neq 0$ around one given site.

Therefore, for a single electron one is restricted to studying electron energies for two different classes of ionic deformations. Notice that the results quoted above are valid at any lattice dimensionality.

In the case of the Bethe lattice, a Dyson equation for the local propagator can be written in the adiabatic limit,

$$\left(\omega+g'X_i-\frac{t^2}{4}\sum_j G_{j,j}\right)G_{i,i}=1, \tag{A4}$$

then the electronic energy can be derived from the knowledge of the adiabatic electron propagator, which is the solution of Eq. (A4) for a given set of deformations $\{X_i\}$.

In case (a) (delocalized solution) the solution is trivially the free-electron propagator in the Bethe lattice. The ground-state electron energy is then $E_{\rm el}=-t$.

In case (b) (localized solution) the $d\to\infty$ limit together with Eq. (A3) implies that only one site is appreciably distorted. Calling 0 the center-of-deformation site it is easy to see that the nearest-neighbor deformation is of the order $1/d$, the next-nearest-neighbor deformation is $1/d^2$, and so on, so that the total charge can be spread on several shells of neighbors even in the $d\to\infty$ limit. The main simplification of the $d\to\infty$ limit is then that the elastic energy *is solely determined by the* 0*-site deformation*, for it depends on X_i^2. Consequently we have two kinds of local propagators: one that propagates the electron from site 0 back to site 0, which depends upon the deformation

$$G_{0,0}=\frac{1}{\omega+g'X_0-(t^2/4)G} \tag{A5}$$

and one that propagates the electron from any to any other site, which is free

$$G=\frac{1}{\omega-(t^2/4)G}. \tag{A6}$$

In the case (b) a pole in the local Green's function of Eq. (A5) emerges out of a band. The position of such a pole determines the electronic ground state energy. Using Eqs. (A5) and (A6) we get the following equation:

$$E_{\rm el}+g'X_0-\tfrac{1}{2}{\rm Re}(E_{\rm el}-\sqrt{E_{\rm el}^2-t^2})=0, \tag{A7}$$

whose solution is

$$E_{\rm el}/t=-1 \quad \text{for } x<1/2, \tag{A8}$$

$$E_{\rm el}/t=-\frac{1}{4x}-x \quad \text{for } x>1/2, \tag{A9}$$

where $x=g'X_0/t$. We see that near the zero deformation state $x=0$ the two possible solutions (a) and (b) coincide. The total potential (rescaled to the hopping energy t) we need to minimize in order to get the ground-state energy is obtained by adding to the solutions (a) and (b) the elastic term [which is zero in case (a)]. Namely,

$$V_{\rm ad}^{(a)}=\frac{x^2}{4\lambda}-1, \tag{A10}$$

while in case (b)

$$V_{\rm ad}^{(b)}=\frac{x^2}{4\lambda}-1 \quad \text{for } x<1/2, \tag{A11}$$

$$V_{\rm ad}^{(b)}=\frac{x^2}{4\lambda}+\frac{1}{4x}+x \quad \text{for } x>1/2\,; \tag{A12}$$

the result is plotted in Fig. 3. There are three different regimes determined by the following critical values for the coupling constant λ: $\lambda_c'=0.650,\ldots$ and $\lambda_c=0.844,\ldots$: (i) $\lambda<\lambda_c'$—the delocalized solution is the stable minimum. (ii) $\lambda_c'<\lambda<\lambda_c$—the delocalized solution is the stable minimum coexisting with a metastable minimum in the potential $V^{(b)}$, characteristic of the localized solution. (iii) $\lambda>\lambda_c$—the localized solution is the stable minimum.

In the latter case the delocalized solution corresponds to a continuum of unrenormalized excited adiabatic states (shaded area in the lower panel of Fig. 14).

By derivatives of the ground-state energy we obtain the relevant properties of the adiabatic ground state as functions of the coupling constant. All these functions can be expressed in terms of the derivative of the ground-state energy $E_0=V_{\rm ad}(X=X_{\rm min})$ with respect to the scaled coupling parameter x, namely, $\Delta=dE_0/dx$.

The local electron-displacement correlation function and the electron kinetic energy are determined by deriving the ground-state energy (Sec. II)

$$C_0/2\alpha=-\Delta, \tag{A13}$$

$$E_{\rm kin}/t=-E_0+x\Delta. \tag{A14}$$

Finally, the elastic energy is calculated as a derivative with respect to ω_0 and scaled to that parameter so as to get a finite result in the adiabatic limit

$$E_{\rm ph}/\omega_0=-x\Delta. \tag{A15}$$

*Present address: CNRS-LEPES Grenoble, 25 avenue des Martyrs, BP 166, 38042 Grenoble Cedex 9, Grenoble, France.

[1] S. V. Tiablikov, Zh. Eksp. Teor. Fiz. **23**, 381 (1952).
[2] T. Holstein, Ann. Phys. (Leipzig) **8**, 325 (1959); **8**, 343 (1959).
[3] *Lattice Effects in High Temperature Superconductors*, edited by Y. Bar-Yam, J. Mustre de Leon, and A. R. Bishop (World Scientific, Singapore, 1992).
[4] A. J. Millis, P. B. Littlewood, and B. I. Shraiman, Phys. Rev. Lett. **74**, 5144 (1995).
[5] T. A. Tyson, J. Mustre de Leon, S. D. Conradson, A. R. Bishop, J. J. Neumeier, H. Röder, and Jun Zang, Phys. Rev. B **53**, 13 985 (1996).
[6] Y. Yamada, O. Hino, S. Nohdo, R. Kanao, T. Inami, and S. Katano, Phys. Rev. Lett. **77**, 904 (1996).
[7] Y. H. Kim, C. M. Foster, A. J. Heeger, S. Cox, and G. Stucky, Phys. Rev. B **38**, 6478 (1988).
[8] C. Taliani, R. Zambone, G. Raum, F. C. Matacotta, and K. I. Pokhadnya, Solid State Commun. **66**, 487 (1988).
[9] S. Lupi, P. Calvani, M. Capizzi, P. Maselli, W. Sadowski, and E. Walker, Phys. Rev. B **45**, 12 470 (1992); P. Calvani, M. Capizzi, S. Lupi, P. Maselli, A. Paolone, and P. Roy, *ibid.* **53**, 2756 (1996).
[10] A. Bianconi, M. Missori, H. Oyanagi, H. Yamaguchi, D. H. Ha, Y. Nishiara, and S. Della Longa, Europhys. Lett. **31**, 411 (1995).
[11] L. D. Landau and S. I. Pekar, Zh. Eksp. Teor. Fiz. **16**, 341 (1946).
[12] I. G. Lang and Yu. A. Firsov, Zh. Eksp. Teor. Fiz. **43**, 1843 (1962) [Sov. Phys. JETP **16**, 1301 (1963)].
[13] A. S. Alexandrov and J. Ranninger, Phys. Rev. B **45**, 13 109 (1992); Physica C **198**, 360 (1992).
[14] A. A. Gogolin, Phys. Status Solidi B **109**, 95 (1982).
[15] A. S. Alexandrov and H. Capellmann, Phys. Rev. B **43**, 2042 (1991).
[16] T. D. Lee, F. Low, and D. Pines, Phys. Rev. **90**, 297 (1953).
[17] D. Emin, Adv. Phys. **22**, 57 (1973); D. Emin and T. Holstein, Phys. Rev. Lett. **36**, 323 (1976).
[18] D. Feinberg, S. Ciuchi, and F. de Pasquale, Int. J. Mod. Phys. B **4**, 1317 (1990); F. de Pasquale, S. Ciuchi, J. Bellissard, and D. Feinberg, Rev. Solid State Sci. **2**, 443 (1988).
[19] V. V. Kabanov and O. Yu. Mashtakov, Phys. Rev. B **47**, 6060 (1993).
[20] H. de Raedt and Ad Lagendijk, Phys. Rev. B **30**, 1671 (1984).
[21] A. Georges and G. Kotliar, Phys. Rev. B **45**, 6479 (1992).
[22] M. Jarrell, Phys. Rev. Lett. **69**, 168 (1992).
[23] P. G. J. Van Dongen and D. Vollhardt, Phys. Rev. Lett. **65**, 1663 (1990).
[24] A. Georges, G. Kotliar, W. Krauth, and M. J. Rozenberg, Rev. Mod. Phys. **68**, 13 (1996).
[25] S. Ciuchi, F. de Pasquale, C. Masciovecchio, and D. Feinberg, Europhys. Lett. **24**, 575 (1993).
[26] S. Ciuchi, F. de Pasquale, C. Masciovecchio, and D. Feinberg, in *Superconductivity and Strongly Correlated Electron Systems*, edited by C. Noce, A. Romano, and G. Scarpetta (World Scientific, Singapore, 1994), p. 58.
[27] J. K. Freericks, Phys. Rev. B **50**, 748 (1994).
[28] J. K. Freericks, M. Jarrell, and D. J. Scalapino, Phys. Rev. B **48**, 6302 (1993).
[29] J. K. Freericks and M. Jarrell, Phys. Rev. Lett. **75**, 2570 (1995).
[30] A. J. Millis, R. Mueller, and B. I. Shraiman, Phys. Rev. B **54**, 5389 (1996).
[31] S. Ciuchi, F. de Pasquale, and D. Feinberg, Europhys. Lett. **30**, 151 (1995).
[32] H. de Raedt and Ad Lagendijk, Phys. Rev. Lett. **49**, 1522 (1982); Phys. Rev. B **27**, 6097 (1983).
[33] F. Marsiglio, Phys. Lett. A **180**, 280 (1993); Physica C **244**, 21 (1995).
[34] M. Capone, M. Grilli, and W. Stephan (unpublished).
[35] T. Hotta and Y. Takada, Phys. Rev. Lett. **76**, 3180 (1996).
[36] Concerning the generality of the $d\to\infty$ Holstein model, let us remark that a dispersionless phonon spectrum is quite generic in infinite dimensions. Actually, if we consider a hypercubic lattice of linked springs the elastic constant K must be scaled as $K=K^*/d$ in order to obtain a finite elastic energy per oscillator. The resulting acoustic spectrum has a dispersion given by $\omega_{\mathbf{k}}^2=\omega_0^2[1-(1/d)\Sigma_{n=1}^{d}\cos k_n]$ where $\mathbf{k}=(k_1,\ldots,k_d)$ is the wave vector if we choose a unit spacing. Except some special vectors such as $\mathbf{k}=(0,0,\ldots,0)$ or $(\pi,\pi,\ldots,\pi)$, the summation disappears as $1/\sqrt{d}$ in the limit of infinite d. In other words, the spectral weight of lattice phonons becomes a delta peak at a finite frequency $\omega_0^2=K^*/M$.
[37] G. D. Mahan, *Many-Particle Physics* (Plenum Press, New York, 1990), Chaps. 4 and 6, and references cited therein.
[38] W. Metzner and D. Vollhardt, Phys. Rev. Lett. **62**, 324 (1989).
[39] S. Engelsberg and J. R. Schrieffer, Phys. Rev. **131**, 993 (1963).
[40] For $d>4$ the shape of the band enters in the determination of the effective mass that increases with λ as $\lambda\gamma$.
[41] $k_d=\int_0^\infty dx x^{d/2-1}/(1+x)^2$.

[42] E. Cappelluti and L. Pietronero, Phys. Rev. B **53**, 932 (1996).
[43] The case $d=2$ is marginal and we cannot gain any insight from the second order perturbation theory.
[44] E. Cappelluti (private communication).
[45] E. V. L. de Mello and J. Ranninger (unpublished).
[46] E. Muller-Hartmann, Z. Phys. B **74**, 507 (1989).
[47] E. N. Economou, *Green's Functions in Quantum Physics* (Springer Verlag, Berlin, 1983).
[48] M. Cini and A. D'Andrea, J. Phys. C **21**, 193 (1988).
[49] V. S. Viswanath and G. Müller, *The Recursion Method* (Springer-Verlag, Berlin, 1994).
[50] A. B. Migdal, Zh. Eksp. Teor. Fiz. **34** (1958) [Sov. Phys. JETP **7**, 996 (1958)].
[51] D. Vollhardt, in *Correlated Electron Systems*, edited by V. J. Emery (World Scientific, Singapore, 1992).
[52] *Handbook of Mathematical Functions*, edited by M. Abramowitz and I. A. Stegun (Dover Publications, New York, 1972).
[53] R. P. Feynman, *Statistical Mechanics: A Set of Lectures* (Addison-Wesley, Redwood City, 1972).
[54] B. Gerlach and H. Löwen, Phys. Rev. B **35**, 4291 (1987); H. Löwen, *ibid.* **37**, 8661 (1988).
[55] Notice that if α^2 is fixed increasing λ means going toward a large phonon frequency limit.
[56] Notice that in this limit $\lambda \to \infty$ while in the adiabatic limit of the Appendix λ is finite.
[57] See, for example, the review F. Yonezawa and K. Morigaki, Prog. Theor. Phys. Suppl. **53**, 3 (1973).